

Designer quantum matter in van der Waals heterostructures

Jose L. Lado and Peter Liljeroth

Department of Applied Physics, Aalto University, FI-00076 Aalto, Finland.

Van der Waals materials can be easily combined in lateral and vertical heterostructures, providing an outstanding platform to engineer elusive quantum states of matter. However, a critical problem in material science is to establish tangible links between real materials properties and terms that can be cooked up on the model Hamiltonian level to realize different exotic phenomena. Our review aims to do precisely this: we first discuss, in a way accessible to the materials community, what ingredients need to be included in the hybrid quantum materials recipe, and second, we elaborate on the specific materials that would possess the necessary qualities. We will review the well-established procedures for realizing 2D topological superconductors, quantum spin-liquids and flat bands systems, emphasizing the connection between well-known model Hamiltonians and real compounds. We will use the most recent experimental results to illustrate the power of the designer approach.

I. INTRODUCTION

Two-dimensional materials are at a focus of intense research efforts, with the paradigmatic examples of graphene, hexagonal boron nitride, transition metal dichalcogenides, and transition metal trihalides. The genuine interest in these materials stems from the many high-quality synthesis possibilities, together with the richness of different behaviours. These compounds have been shown to realize properties starting from conventional insulating and metallic behaviour, all the way up to complex many-body ground states such as superconductors and topological insulators.

Besides their intrinsically interesting properties, layered 2D vdW materials can be easily combined in lateral and vertical heterostructures. As the layers only interact via the weak vdW forces, the individual layers can retain their intrinsic properties. This property alone allows creating combinations of electronic orders that no naturally occurring material possesses. This possibility has given birth to the field designer quantum materials, where heterostructures are exploited to realize elusive quantum phases of matter not present in conventional compounds. In this review, we present a quantum materials cookbook point of view on how to achieve this and use three elusive quantum states engineered in vdW heterostructures as examples: topological superconductors, quantum spin-liquids and flat band systems.

The creation of topological superconductivity represents the first paradigmatic example of the possibilities brought by this flexibility. It is well known that topological superconductivity can be artificially engineered by combining s-wave superconductivity, spin-orbit effects, and magnetism. Materials with these properties can be combined in heterostructures of 2D materials by using layered superconductors, monolayer magnetic materials, and strong spin-orbit effects as the necessary ingredients of realizing topological superconductivity.

A second example consists of engineered quantum spin-liquids, highly entangled quantum magnets. The emergence of quantum spin-liquids is known to require a fine-

tuning between spin-interactions, which is one of the limitations to finding them in non-tunable compounds. VdW heterostructures provide a way around this, with their possibility of finely tuning magnetic interactions in a two-dimensional magnet by a proper choice of 2D substrate. We will also discuss the prospects of realizing QSL in artificial systems.

Finally, as the third example, we discuss how combining two-dimensional materials allow us to create dramatically new electronic dispersions beyond simple superposition of the electronic orders of parent compounds. The most dramatic case of this consists of the emergence of flat bands from a material with highly dispersive electrons. This is exemplified by structurally engineered on-surface graphene structures, and the whole family of twisted vdW heterostructures.

II. ARTIFICIAL VDW TOPOLOGICAL SYSTEMS

The engineering of novel topological states of matter[1, 2] represents one of the milestones of current materials engineering. While a variety of natural topological compounds have been identified in nature[3], artificial engineered systems open new prospects for potential technological applications with common compounds. Ultimately, this topological engineering can ultimately lead to the realization of states that no natural compound hosts. Topological states of matter encompass a wealth of states, including crystalline, higher-order and quasiperiodic topological states. Here, we will focus on two paradigmatic cases, namely quantum anomalous Hall insulators[4] and topological superconductors[5]. These two topological states represent critical milestones for the fields of electronics and topological quantum computing, respectively.

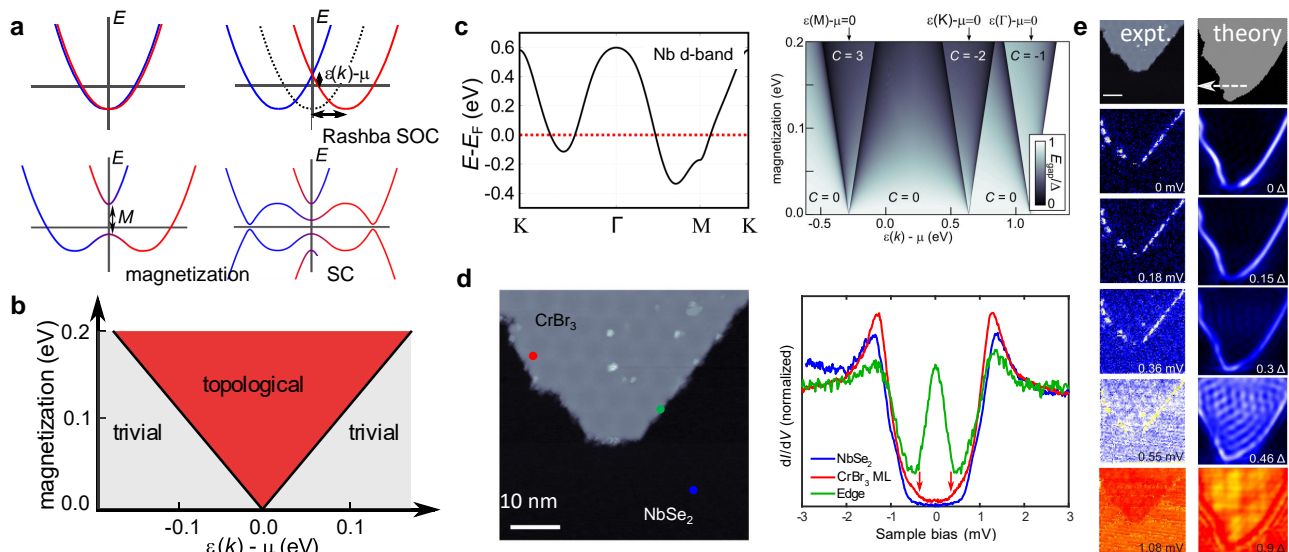


FIG. 1. (a) Schematic of the band structure with the “ingredients” of topological SC: Rashba-type spin-orbit coupling, magnetization, and superconductivity. (b) Resulting topological phase diagram. (c) Nb d-band band structure in NbSe₂ and the topological phase diagram in this system with a triangular lattice [6]. (d) Realization of the TSC in a van der Waals heterostructure. Left panel shows an STM topographic image of a CrBr₃/NbSe₂ heterostructure and dI/dV spectroscopy on the three spots indicated is shown in the right panel [6]. (e) LDOS maps compared with theoretical modelling showing the presence of Majorana zero modes at the island edges [6].

A. Artificial topological superconductors

The creation of topological superconductivity[7] represents the first paradigmatic example of the milestones of artificial engineering[5]. It is well known that topological superconductivity can be artificially engineered by combining s-wave superconductivity, spin-orbit effects, and magnetism[5, 8–12]. Materials with these properties can be combined in heterostructures of 2D materials[13] by using layered superconductors[14], monolayer magnetic materials[15, 16], and strong spin-orbit effects as the necessary ingredients to realize topological superconductivity.

Topological superconductivity represents one of the most pursued quantum states of matter in modern condensed matter physics. Besides the interest in this state sparked from the rise of topological insulators, topological superconductors represent one of the potential cornerstones for topological quantum computing[17–19]. However, topological superconductors are extremely rare in nature, and thus a great amount of experimental efforts have been focused on engineering this state in a variety of platforms[5, 12]. The fundamental requirements for creating topological superconductivity rely on creating an effective superconducting spin-triplet state[7, 20] starting from a conventional spin-singlet s-wave superconductor. This can be achieved by creating fine-tuned spin textures in materials combining exchange fields and strong Rashba spin-orbit coupling. Based on this idea, a variety of proposals and realizations have been demonstrated in the last years in semiconducting nanowires[9, 19, 21, 22],

atomically engineered chains [23–30] and topological insulators[10, 31]. In all these systems, the critical emphasis is put on combining different materials containing magnetism and superconductivity, a task in which interface physics is known to play a critical role[32]. Two-dimensional materials provide a unique opportunity in this direction, due to the weak van der Waals forces that allow combining different layers[13, 16], namely superconducting and magnetic, on a single van der Waals heterostructure.

The requirement of these different order parameters to engineer a topological superconductor can be easily rationalized. In short, engineering topological superconductivity requires creating an effective spinless superconductor, whose minimal model gives rise to a topological superconducting state. For this sake, let us start with the simplest model for topological superconductivity: the one-dimensional Kitaev model[7]. This model considers spinless electrons on a one-dimensional chain in the presence of a finite first nearest-neighbor pairing, whose Hamiltonian takes the form

$$H = \sum_n t c_n^\dagger c_{n+1} + \sum_n \Delta c_n c_{n+1} + \text{h.c.} \quad (1)$$

It should be noted that for spinless fermions, on-site superconductivity is forbidden from the fermionic anticommutation relations. The previous Hamiltonian in Fourier space takes the form

$$H = \sum_n t \cos(ka) c_k^\dagger c_k + \sum_n \Delta \sin(ka) c_k c_{-k} + \text{h.c.} \quad (2)$$

giving rise to a fully gapped eigenspectra $\epsilon_k = \sqrt{t^2 \cos(ka)^2 + \Delta^2 \sin(ka)^2}$. Despite its fully gapped structure, solving the Hamiltonian Eq. 1 with open boundary conditions gives rise to a zero mode, which in the case of the exactly solvable point $\Delta = t$ has an associated eigenstate of the form $\gamma = \frac{1}{2}(c_0 + c_0^\dagger)$. For finite chemical potential μ , an exponentially localized zero mode exists, yet with a more complex spatial profile. In contrast with conventional fermions, this creation operator is its own dagger $\gamma = \gamma^\dagger$. This implies that these particles are their own antiparticles, which is expressed in this model through this mathematical property, as expected from a Majorana operator. Similar models can be written for a two-dimensional system, in which case the single-Majorana mode becomes a propagating Majorana edge state in an otherwise fully gapped spectrum.

The central question of artificial topological superconductivity is to find procedures of engineering an effective spinless superconductor, starting from spin-singlet superconducting term of the form

$$H = \sum t_{ij} c_i^\dagger c_j + \sum_n \Delta c_{n,\uparrow} c_{n,\downarrow} + \text{h.c.} \quad (3)$$

Many of the strategies to engineer topological superconductivity rely on designing a pseudo-helical electron gas[9, 10] (states crossing the Fermi level have a spin that is locked to their momentum, i.e. a certain momentum implies certain spin direction), yielding an effective single degree of freedom and with a finite projection on the spin-singlet state above, which interestingly could be directly engineered with two-dimensional van der Waals topological insulators[33]. The previous idea implies that the electronic modes must have a finite spin-momentum coupling so that the propagation direction depends on the spin channel. Such spin-momentum coupling can be realized by different forms of spin-orbit coupling[9, 10], or by exploiting non-collinear magnetic textures[23, 34]. It is interesting to note that these strategies work both in one and two-dimensions, and as a result, recipes for one-dimensional topological superconductivity can easily be generalized to two dimensions.

The typical recipe for achieving topological superconductivity is illustrated in Fig. 1a. Starting with a parabolic band, the addition of Rashba-type spin-orbit coupling and magnetization creates the type of band structure required for TSC as explained above. The addition of superconductivity completes the requirements and results in a system that realizes the phase diagram shown in Fig. 1b. When the chemical potential is tuned to the band crossing point at $k = 0$, even a very small magnetization is sufficient to drive the system into the topological phase. If the chemical potential is tuned away from this point, then stronger magnetization is needed. Although this procedure requires very precise fine-tuning between the system parameters, it has been successfully demonstrated for a variety of semiconductor devices[21, 22], and

van der Waals materials[6]. Finally, it is worth emphasizing that besides the Majorana edge modes, topological superconductors are also expected to show Majorana excitations at domain walls[35, 36] and vortices[37–40].

B. Materials for artificial topological superconductors

The section above lays out the rather stringent requirements for realizing topological superconductivity, and we need materials that will retain their magnetic and superconducting properties in a heterostructure. This strongly suggests using vdW materials: this allows for a rational design of the heterostructure as we expect to retain the intrinsic properties of the different constituents. Topological superconductivity has been realized in atomic-scale structures using conventional materials (e.g. iron atom chains on a lead or rhenium substrates [24–27], cobalt islands under a Pb monolayer, and iron islands on an oxygen-terminated rhenium substrate [32, 41]). However, considering the strong chemical bonding between the materials in this case, these systems are susceptible to disorder, and interface engineering might be required in some cases [32].

While many monolayer ferromagnet materials are available for exfoliation (e.g. CrI₃), they are very reactive, and accessing the topological edge modes in scanning probe microscopy and other experiments requires the system to have very clean edges. This points out towards the use of e.g. molecular-beam epitaxy (MBE) growth and luckily high-quality growth of several materials has been demonstrated (Fe₃GeTe₂ [42], CrBr₃ [43, 44]). For the superconductor material, typical suggestions would include the 2H phase of the NbS₂, NbSe₂, TaS₂, and TaSe₂ [45, 46]. The scheme for realizing TSC is also applicable to bulk superconducting substrates, there the magnetic layer will couple strongly to the top layer of the SC, and as long as the substrate has relatively weak interactions between the layers, it is expected to work similarly to the monolayer case [6, 47]. These real materials have hexagonal symmetry, which is reflected in the band structure. Instead of a single high-symmetry point in the Brillouin zone, there are several (Γ , M , and K points), and the topological superconducting phase can be realized at any of these points. This means that tuning the Fermi level across the relevant band (e.g. the Nb d-band in the case of NbSe₂), there are three different topological phases that have different Chern numbers as illustrated in Fig. 1c. In a real vdW heterostructure, the doping of the substrate will determine whether the system will enter a topological phase.

This route to TSC has been realized experimentally in CrBr₃ / NbSe₂ heterostructures [6, 44]. As can be seen from the calculated Nb d-band bandstructure shown in Fig. 1c, the M point is closest to the Fermi level, and it is likely that the topological phase arises from this point. Experimentally, the strongest signature is the

Majorana edge modes that appear at the interface between the trivial and topological phases. This is shown in Fig. 1d, which shows an STM topographic image of CrBr₃ island on a bulk NbSe₂ substrate and three dI/dV spectra (the signal is proportional to the local density of states, LDOS, at the position of the STM tip): on the NbSe₂ substrate (blue), on the CrBr₃ island (red) and right at the edge of the island (green). The spectrum recorded on the island edge has a strong peak centered around the Fermi level (zero bias) consistent with the expected LDOS corresponding to the Majorana zero modes. Fig. 1e shows the measured (left) and theoretical LDOS (right) as a function of the energy. At the Fermi energy, both the bulk phases are gapped, and only the Majorana modes at the edges of the islands are visible. As the energy is increased, we eventually start to see excitations in the topological superconductor with the edge modes overlapping with bulk states. Finally, above the superconducting gap, all significant LDOS contrast is lost.

Comparison between theory and experiment allowed estimating the values of the model parameters, namely, the induced magnetization in the top NbSe₂ layer due to the proximity of the CrBr₃ layer and the magnitude of the Rashba spin-orbit coupling. These estimates suggest that the magnetization and the spin-orbit coupling are of a similar magnitude, a few tens of meV. This values were also consistent with density-functional theory (DFT) calculations and in-line with proximity induced exchange coupling in CrI₃/WSe₂ and CrBr₃/MoSe₂ heterostructures [48, 49]. Finally, the moiré pattern between CrBr₃ and NbSe₂ was suggested to further stabilize the topological superconducting state[50].

C. Artificial Chern insulators

Chern insulators [54] represent another paradigmatic state of matter in two-dimensional systems. Besides their conventional engineering by combining spin-orbit coupling and exchange fields [4], van der Waals materials offer a novel approach to engineered Chern insulators. This new approach to engineer Chern bands specifically exploits moiré patterns in twisted two-dimensional materials. The emergence of flat bands stems from a non-abelian elastic gauge field and will be further addressed in more detail in section IV E. As illustrated in Fig. 2a-c, the varying lattice registry in twisted bilayer graphene creates a long-wavelength moiré pattern. This moiré modulation creates moiré mini-Brillouin zones at the K and K' points of the two graphene layers. These valleys are well-separated, and each valley hosts two Dirac cones of the same chirality. The Dirac cones living at the K^1 and K^2 (and at K'^1 and K'^2) hybridize, and when the respective Dirac points are sufficiently close to each other in the k -space, this hybridization results in the formation of a flat band with narrow bandwidth that is well separated from other bands is formed as the twist angle θ is tuned across the magic angle (Fig. 2c). This emergence of flat

bands in twisted graphene bilayers is the starting point for realizing the Chern insulator states[55, 56].

Flat bands in twisted bilayers can be interpreted as pseudo-Landau levels of an artificial gauge field, generated by the modulated stacking in the unit cell[57]. Close to charge neutrality, these flat bands yield an 8-fold manifold, two-fold degeneracy coming from electron-hole states, two-fold coming from valley symmetry and two-fold coming from spin[55, 56, 58, 59]. As Landau levels[57, 60], each flat band is expected to carry a non-trivial Chern number, analogous to conventional Landau levels of quantum Hall states[61]. However, the original system is time-reversal symmetric, implying that flat bands stemming from opposite valleys will carry opposite Chern numbers[57, 62]. This property suggests that if valley symmetry is spontaneously broken, for example, due to electronic interactions, twisted graphene bilayers become natural Chern insulators[63]. The breaking of valley symmetry takes place when electronic interactions create a spontaneous symmetry breaking, leading to a filling of just on the the valley flat bands. A specific feature that must be taken into account is that due to the existence of Dirac points in the electronic structure[55, 56, 58, 59], leading to the Chern insulator regime requires to first opening a gap at the Dirac points[63–65]. This is done by taking aligned hBN layers with the twisted bilayer that induce a small symmetry breaking in the twisted bilayer lifting the original Dirac points. Ultimately, in the presence of partial filling, this could lead to the emergence of fractional Chern states [66].

D. Materials for artificial Chern insulators

These predictions were realized in twisted graphene bilayers with the twist angle ($\theta = 1.15^\circ$) tuned to yield flat bands in the electronic spectrum [53, 55, 56]. The sample fabrication followed the usual “tear and stack” process [52, 67, 68], but TBG was aligned with the underlying h-BN layer. The alignment with BN turns out to be critical in lifting the low energy Dirac points, allowing for the emergence of a valley polarized state. These state-of-the-art devices typically use TBG encapsulated by h-BN layers, and atomically smooth graphite flake is used as the gate electrode (see Fig. 2a). Finally, the stack is electrically contacted using so-called edge contacts, which have high transparency and avoid unwanted doping of the TBG [51]. Fig. 2d shows the longitudinal (R_{xx}) and the Hall (R_{xy}) resistances measured as a function of the carrier density on a magic angle TBG device at $T = 1.6$ K and under an external magnetic field of $B = +150$ mT [53]. As expected for a quantum Hall state, R_{xy} reaches h/e^2 and R_{xx} approaches zero when the electron density is tuned to filling factor $\nu = 3$ (ν , where ν is the number of the electrons in the flat band per moiré unit w.r.t. no external doping, i.e. ν can have values between -4 and 4). The previous phenomena

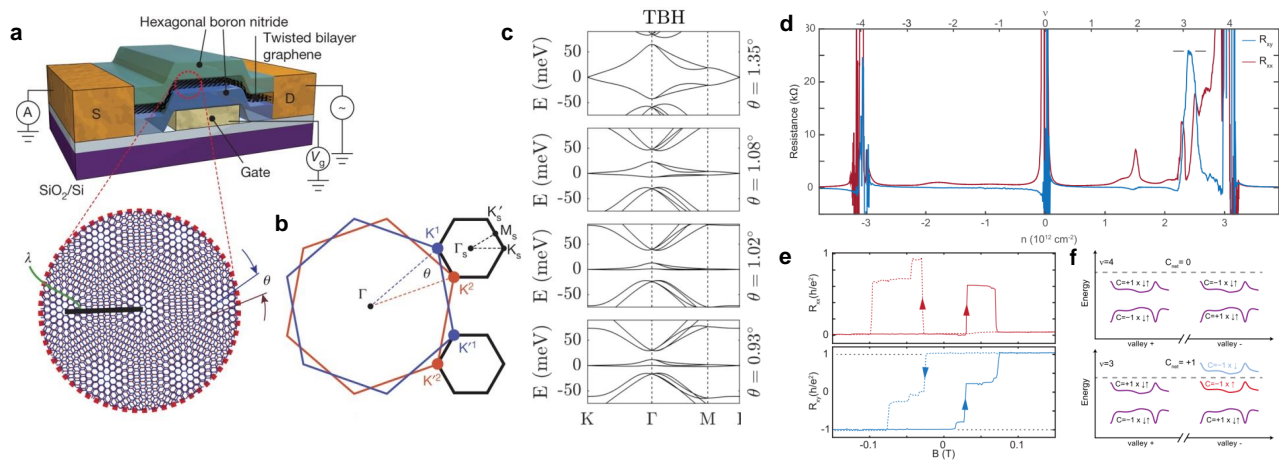


FIG. 2. Chern insulating states in twisted bilayer graphene. (a) Illustration of a typical state-of-the-art device for TBG transport experiment. TBG is sandwiched between two layers of h-BN and atomically smooth graphite flake is used as the gate electrode. The contacts are so called edge contacts that have high transparency and avoid unwanted doping of the TBG [51]. (b) The moiré modulation creates moiré mini-Brillouin zones at the K and K' points of the two graphene layers. These valleys are well-separated and each valley hosts two Dirac cones of the same chirality. (c) Evolution of the band structure as the twist angle is tuned. At the magic angle, a flat band with narrow band width that is well separated from other bands is formed. Panels a-c from Ref. [52]. (d) Longitudinal (R_{xx}) and the Hall (R_{xy}) resistances measured as a function of the carrier density on a magic angle TBG device at $T = 1.6$ K and under an external magnetic field of $B = +150$ mT. (e) R_{xx} and R_{xy} measured at the filling factor $\nu = 3$ as a function of magnetic field B . (f) Schematic band structure at full filling of a moiré unit cell ($\nu = 4$) and $\nu = 3$. Panels e-f from Ref. [53].

are the hallmarks of the QAHE state, and most importantly it is retained in the absence of the field as shown in Fig. 2 - The Hall resistivity is hysteretic (Fig. 2e), with a coercive field of several tens of millitesla. The Hall resistivity is quantized ($R_{xy} = h/e^2$) and the longitudinal resistivity remains small through zero external magnetic field, which demonstrates that the quantum anomalous Hall state is stabilized by spontaneously broken time-reversal symmetry. In particular, this time-reversal symmetry breaking is purely associated to the valley sector, where spontaneous symmetry-breaking leads just one of the valley filled as sketched in Fig. 2f. Finally, it is worth to note that it is quite typical in the TBG experiments that the observed phenomena are device-specific, with minor differences in the device parameters being decisive which states are formed. For example, robust, thermally activated, trivial insulator behavior and the QAH state can occur in very similar devices.

Typically, the Chern number can be estimated from the value of the quantized Hall conductance, but this measurement requires working on a transport setup, and it would be extremely interesting to be able to somehow measure the Chern number directly and independently. Precisely this was done by a scanning tunneling microscopy-based technique to directly measure the Chern numbers of the different Chern insulating states [69]. The topological gaps can be identified by measuring the LDOS as a function of the electron density in the system (controlled through external doping) at different external magnetic fields. If the electron density at which gap opening and closing takes place depends on

the external magnetic field, the transition can be identified as a topological transition. Tracking the electron densities at which these transitions happen as a function of the magnetic field B , gives direct access to the associated Chern number C via $\frac{dn}{dB} = C/\Phi_0$, where Φ_0 is the magnetic flux quantum. In addition to a host of levels arising from the zeroth Landau level at $\nu = 0$ with Chern numbers $C = 0, \pm 1, \pm 2, \pm 3, \pm 4, \pm 8, \pm 12$, the authors observe a hierarchy of correlated Chern insulating phases with Chern numbers $C = \pm 1, \pm 2, \pm 3$ emerging as a function of magnetic field from the different filling factors $\nu = \pm 3, \pm 2, \pm 1$, respectively. All these phases are stabilized by a magnetic field.

In addition to the example above, the Chern insulating state and the quantum anomalous Hall effect has also been realized in rhombohedral (ABC-stacked) graphene trilayers and twisted monolayer - bilayer graphene samples [70–72] and recent experiments on magic-angle bilayers also suggest the possibility of realizing fractional Chern insulator states [73].

III. VDW QUANTUM SPIN-LIQUIDS

Quantum spin-liquids [78, 79] are highly entangled quantum magnets, characterized by the emergence of novel fractionalized particles. These many-body states are classified to their pattern of long-range entanglement. In terms of their excitation spectrum, quantum spin-liquids can be classified in gapped or gapless, and in a minimal picture, this is ascribed to a gapless or

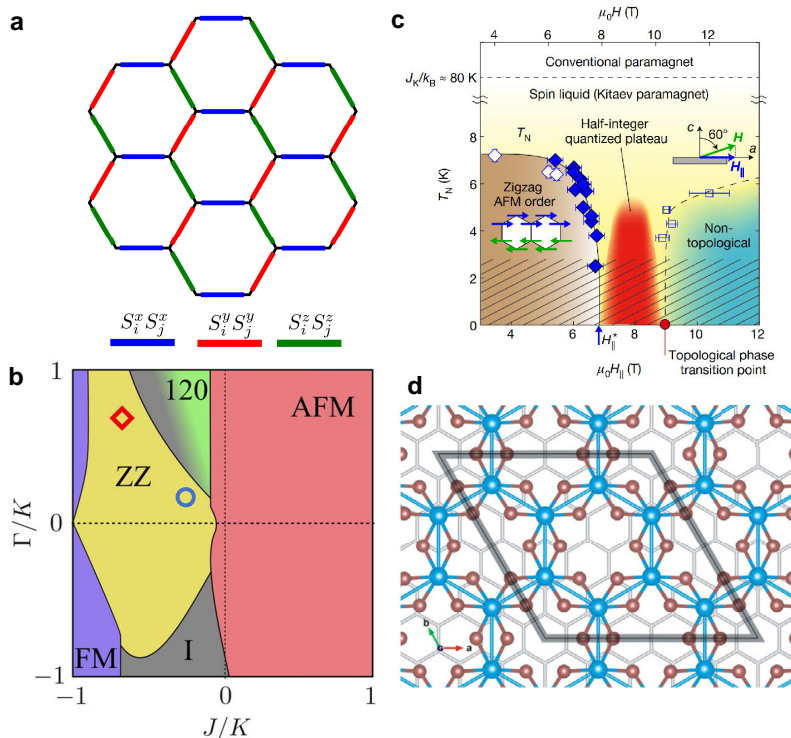


FIG. 3. (a) Sketch of a spin model with frustration stemming from anisotropic interactions. (b) Phase diagram of RuCl₃ [74] taking constant second and third neighbour exchange coupling. The red diamond indicates the estimated parameters for bulk RuCl₃ and the blue circle those for monolayer RuCl₃ on graphene [74–76]. (c) The phase diagram of α -RuCl₃ in an external magnetic field at $\theta = 60^\circ$. Open and closed diamonds represent the onset temperature of zigzag type AFM order based on thermal Hall conductivity measurements. A half-integer quantized plateau of the 2D thermal Hall conductance is observed in the red area and open blue squares represent the fields where the thermal Hall response disappears [77]. (d) Top view of α -RuCl₃/graphene heterostructure, where the blue and maroon spheres represent Ru and Cl atoms, respectively, and the gray hexagon indicates the graphene monolayer [75].

gapped quasiparticle spinon excitations [79–81]. In addition, quantum spin-liquids can be described by a deconfined gauge field theory [79, 82, 83], namely a theory that involves free spinons capable of propagating [84]. A fundamental question is, which mechanisms capable of driving a system from a magnetically ordered state to a quantum disordered one can be designed.

A. QSL from frustrated anisotropic interactions

A first strategy to design quantum spin-liquids is to focus on models showing highly directional interactions that are inherently frustrated [85]. This can be done, for example, by taking square [86] or honeycomb lattices [85], and imposing anisotropic spin-spin interactions that are dependent on the bond considered. As magnetic interactions in materials are rotational symmetric in the absence of spin-orbit coupling, these mechanisms are expected to be realized in materials containing heavy atoms in which spin-orbit effect compete and even overcome other interactions present [87–90].

Due to their interacting nature, the solution of quan-

tum spin-liquid models represents one of the open problems in many-body physics. A great amount of insight can, however, be obtained from finely tuned models that allow for an exact solution. Among these specially tuned models, we encounter the Toric code and the anisotropic Kitaev honeycomb model [85]. In particular, the Kitaev model realizes a highly anisotropic spin model in a honeycomb lattice that takes the form

$$H = \sum_{\langle ij \rangle} S_i^\gamma S_j^\gamma \quad (4)$$

where $\langle ij \rangle$ denote first neighbors and γ labels the spin-component that interacts for each bond as depicted in Fig. 3(a). The genuine feature of the Kitaev honeycomb model stems from the possibility of obtaining an exact solution in terms of single particle excitations. Remarkably, the single-particle excitations are of Majorana type, and depending on the parameter regime, realize gapless or gapped Majorana states [85].

B. Experiments QSL with anisotropic interactions

Interestingly, the Kitaev honeycomb model [85] (illustrated in Fig. 3a) can be potentially adiabatically connected to quantum spin-liquid states realized in α - RuCl_3 (RuCl_3) [74, 89, 91–93], and thus in the following we will focus on this compound. RuCl_3 is a layered Mott insulator with significant spin-orbit interactions that is in the close proximity to the quantum spin-liquid ground state [66, 74, 75]. However, these materials often host complex Hamiltonians having several contributions beyond the Kitaev exchange, including first, second and third neighbor exchange, and symmetric off-diagonal exchange [74, 94–96]. The model typically employed for this compound gives rise to the phase diagram sketched in Fig. 3b as a function of the first neighbor couplings, keeping the second and third neighbor exchange finite [74]. In Fig. 3b, the x-axis represents the ratio of the Heisenberg (J) to Kitaev-type (K) spin coupling and Γ is symmetric off-diagonal exchange coupling. The whole diagram has been evaluated with the ratio of Hund's coupling (J_H) to the Coulomb on-site interaction (U) of $J_H/U = 0.2$, which can be estimated from ab initio calculations. It can be seen that the phase diagram hosts ordered magnetic phases ranging from ferromagnetic (FM) and antiferromagnetic (AFM) to more complicated zigzag (ZZ), 120 and incommensurate order (I) phases, even without considering variations in the further neighbor exchange. The best estimate for the parameters corresponding to bulk RuCl_3 is shown as a red diamond. This implies that the ground state of RuCl_3 is actually an ordered magnetic phase, which has been experimentally confirmed using, e.g., thermal Hall conductance measurements [77].

Remarkably, it was experimentally demonstrated that applying a sufficient in-plane magnetic field can destroy the long-range order of the magnetic ground state and give rise to quantum spin-liquid behaviour [77]. This is illustrated in the phase diagram shown in Fig. 3c, where the boundaries of the different phases have been followed using thermal Hall conductance measurements. Interestingly, the Majorana edge modes that arise in the quantum spin-liquid ground state can be directly verified as half-integer quantized thermal conductance, which is observed in the region shaded with red in Fig. 3c. Further increasing the lateral magnetic field gives rise to a phase transition to some other non-topological phase.

In addition to the application of a lateral magnetic field, many other routes (e.g. external pressure and chemical doping) are being tested to suppress magnetism, enhance the pure Kitaev interactions and drive the system towards the quantum liquid state. In the spirit of the designer material principles, we highlight a couple of theoretical ideas where heterostructures could be used to promote the quantum spin-liquid state. It has been proposed that monolayer RuCl_3 on graphene (illustrated in Fig. 3d) would result in a system with enhanced Kitaev type interactions [75, 76]. By using ab initio calculations, it was shown that the RuCl_3 becomes strained

and doped in this heterostructure. This might even drive an insulator-to-metal transition and help to realize predicted, exotic superconducting states in quantum spin-liquids [75, 101]. In any case, the strain and doping are predicted to enhance the Kitaev interactions (increasing K and decreasing J and Γ) and move the system closer to the Kitaev. RuCl_3 /graphene heterostructures have been also realized experimentally [102, 103], but not yet down to the monolayer limit. However, experiment on thicker RuCl_3 layers already give indications of the charge transfer and hybridization between the RuCl_3 and graphene bands [102, 103].

C. QSL from geometric frustration

Geometric frustration can lead to spin-liquid behavior and considering a simple picture of three spins can give a flavor of the general idea: Consider three spins at the corners of a triangle with antiferromagnetic interactions. This system does not have a configuration where all antiferromagnetic interactions can be simultaneously satisfied, i.e. the system is frustrated. This geometric frustration leads to unusually large ground state degeneracies, already at the classical level. The situation described above corresponds to a classically frustrated system, in which quantum entanglement between sites is not considered and corresponds to the so-called spin ice models. In the quantum realm, an effective strategy to realize quantum spin-liquid physics is to focus on models realizing non-bipartite lattices, such as triangular and kagome lattices. Kagome lattice models [104–106] have been known to be a paradigmatic platform for quantum spin-liquid physics. Since triangular lattices are often more common in the van der Waals world, we will in the following focus on that case. Focusing on the triangular lattice model, in the minimal case in which only first neighbor interactions are considered, the ground state is actually an ordered state with 120 degrees spin spiral [107–109]. However, this model can be pushed to a more frustrated regime by including additional interactions [110, 111], and in particular, a second neighbor exchange coupling [112], driving the system to a quantum spin-liquid ground state. Although an exact solution cannot be obtained in this limit, tensor network calculations have shown strong signatures of a gapless QSL liquid state in this regime, featuring gapless Dirac spinons. [112]

The low energy excitations of these models in terms of chargeless emergent fractionalized excitations with $S = 1/2$ known as spinons. We start with a Heisenberg model of the form $H = \sum_{ij} J_{ij} \vec{S}_i \cdot \vec{S}_j$ where S_i are the local spin operators. Assuming a quantum spin-liquid ground state, we can express the localized spins as emergent chargeless $S = 1/2$ fermions of the form $S_i^\alpha = \sum_{s,s'} \sigma_{s,s'}^\alpha f_{i,s}^\dagger f_{i,s'}$, where $f_{i,s}^\dagger$ denotes the creation operator of a fermionic spinon in site i , and $\sigma_{s,s'}^\alpha$ are the spin Pauli matrices. The localized moment is implemented by enforcing having a

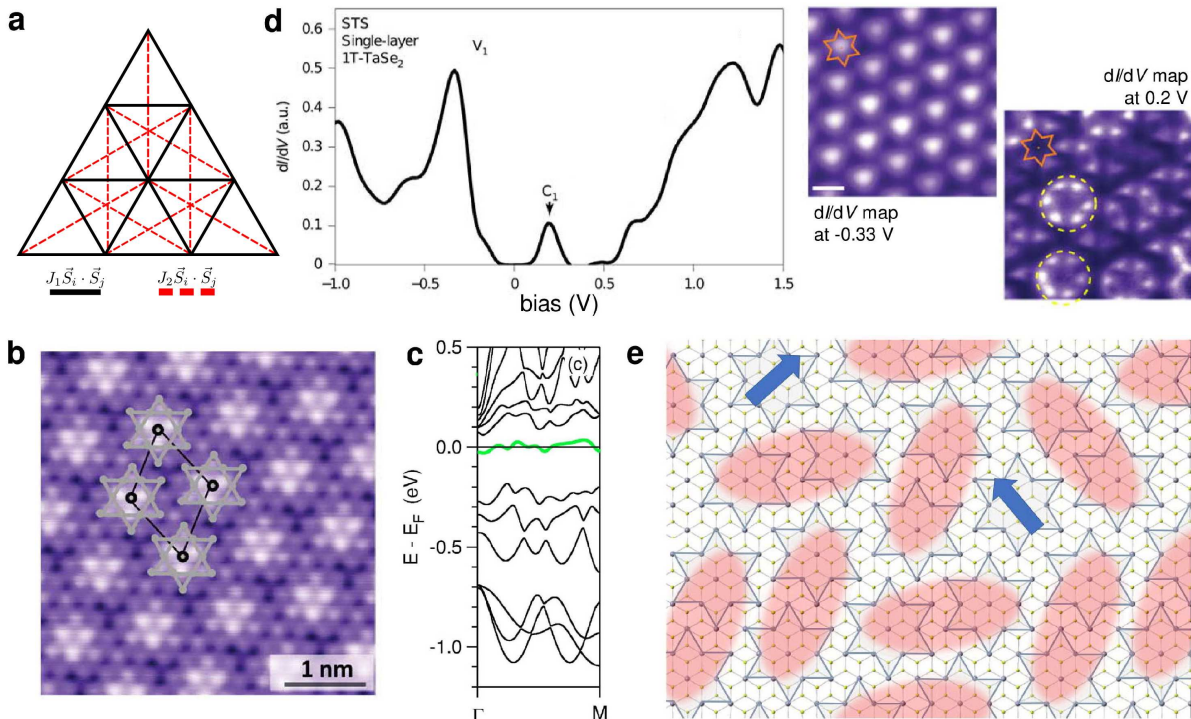


FIG. 4. (a) Schematic of a quantum-spin-liquid with frustration stemming from geometric frustration. (b) STM image recorded on a buk 1T-TaS₂ surface showing the characteristic “Star-of-David” charge-density wave pattern [97]. (b) Calculated band structure of 1T-TaS₂ with the $\sqrt{13} \times \sqrt{13}$ “Star-of-David” reconstruction and including the Ta spin-orbit coupling reveals a single distinct split-off banb at the Fermi level (green line) [98]. Including the Hubbard U-term splits this band into a lower and upper Hubbard band (d) STM dI/dV measurements on a related compound 1T-TaSe₂ monolayer showing LHB and UHB [99]. The panels on the right show constant height dI/dV maps that allow direct visualization of the LHB and UHB wavefunction symmetries. (e) Illustration of the low-temperature state of 1T-TaS₂ with spatially random pairs of “Star-of-Davids” forming singlets. It is possible to form gapless, low-energy fractional excitations (blue arrows) [100].

single fermion in each site $f^\dagger f = 1$. At the mean field level, the Heisenberg Hamiltonian a tight binding model of free propagating $S = 1/2$ spinons of the form

$$H = \sum_{ij} \chi_{ij} f_{i,s}^\dagger f_{j,s'} \quad (5)$$

where χ_{ij} are the mean-field parameters of the mean-field Hamiltonian. The spinon excitations of the quantum spin-liquid state can thus be understood from the spinon dispersion. For example, gapless Dirac quantum spin-liquids have an associated spinon model featuring Dirac points,[112] whereas models with a finite spinon Fermi surface are stem from model with a finite Fermi surface. This classification is often used when characterizing quantum spin-liquid ground states, and has direct impact on the temperature-dependence of the thermal conductivity[113].

D. Experiments on geometrically frustrated QSLs

The necessary ingredients for a QSL - triangular lattice with frustrated magnetism (Fig. 4a) - can be realized in van der Waals materials. This has been demonstrated in the 1T phase of TaS₂ (1T-TaSe₂ is expected to be similar), where the presence of various charge-density wave (CDW) states (depending on the temperature) has been known for some time [114–116]. The low-temperature CDW state results in a $\sqrt{13} \times \sqrt{13}$ reconstruction of the 1T-TaS₂ lattice that has a 13 Ta atom “star of David” unit cell [97, 98, 114–116] as illustrated in Fig. 4b. This causes folding of the band structure and, together with modified hoppings caused by the reconstruction and the presence of spin-orbit coupling, results in a single band with a relatively flat dispersion at the Fermi level (Fig. 4c) [98]. In the presence of strong electron-electron interactions (U larger than the bandwidth of band at Fermi level), the system will undergo a Mott metal-insulator transition and instead of the single band at the Fermi level, there will be a fully occupied lower Hubbard band (LHB) below the Fermi level and a fully unoccupied upper Hubbard band (UHB) above it

[117].

In the case of 1T-TaS₂, this Hubbard band correspond to a single unpaired electron per CDW “star of David” unit cell, which are the building block of the quantum spin-liquid state in this material. The Hubbard bands have been demonstrated in bulk 1T-TaS₂ [97, 118] and also in monolayer 1T-TaSe₂ [99]. As illustrated for 1T-TaSe₂ in Fig. 4d, tunneling spectroscopy allows direct verification that the system is gapped and the energies of the LHB and UHB can be easily probed. In addition, by mapping the spatial variation of the tunneling conductance $dI/dV \propto \text{LDOS}$, the spatial symmetries of the states can be probed. In the case of 1T-TaSe₂ monolayer, it can be seen that the orbital texture of LHB and UHB are different (right side of Fig. 4d).

While STM and tunneling spectroscopy can be used to probe the Hubbard bands, it is difficult to directly use these techniques to probe the spin-liquid state. This is usually done with neutron scattering, where the “smoking gun” for the QSL state is the lack of magnetic order down to the lowest temperatures. The other option is muon-spin-relaxation, which has been applied to bulk 1T-TaS₂ to show that the spin excitations are gapless, and there is no long-range order in temperatures of at least down to 70 mK [100]. Those experiments show that below 55 K, there is a broad distribution of the relaxation times indicating a highly inhomogeneous magnetic phase at all Ta sites. This is strong evidence that there is growing randomness in the spin system as temperature decreases below 55 K. The observed slowing down of spin fluctuations is consistent with the freezing of singlets as illustrated in Fig. 4e. Interestingly, for 1T-TaS₂ the resonant valence bonds are formed between magnetic moments with an extension of the enlarged unit cell generated by the CDW, in comparison with the atomic-like moments of bulk QSL candidates.

The problem with the bulk probes such as neutron scattering or muon spin-relaxation is that they are typically not sufficiently sensitive to probe monolayer samples. There are theoretical suggestions that tunneling spectroscopy could be used for this even though the magnitude of the predicted signal would depend on the measurement geometry (e.g. 2D junction vs. STM) and the type of the spin-liquid [120]. In addition, and despite their chargeless nature, signatures of spinon interference can be potentially probed by inelastic transport spectroscopy[121]. Finally, muon spin-relaxation has been used to probe the Kondo effect with spinons[122], by probing the existence of a spinon-Kondo cloud around magnetic impurities, and this technique could perhaps be extended to monolayer samples.

IV. NEW VDW FLAT BANDS

The engineering of flat bands has been at the forefront of condensed matter physics for a long time. Flat band systems are characterized by having almost dispersionless

states, which in the presence of any residual interactions are expected to be prone to a variety of electronic instabilities [123–125]. In the following, we will discuss several directions that van der Waals materials provide towards the realization of flat band systems.

A. Generating flat bands from geometric frustration

The simplest instance in which flat bands appear in electronic systems are tailored lattices leading to destructive interference[123, 126]. Paradigmatic examples of these flat band models are Lieb and kagome lattices[126]. In this system, electron propagation is quenched due to the existence of complementary paths that interfere destructively. This destructive interference can be often weakened by adding additional perturbations. For example, next nearest neighbour (NNN) hoppings interactions will often cause the flat bands to acquire dispersion, as flat bands are localized eigenstates on “disconnected” lattice sites and NNN hoppings connect these sites and make the flat band dispersive. In the case of the Lieb lattice, the existence of a flat band can also be understood from Lieb’s theorem[124]. In its general form, this theorem states that for a fully bipartite lattice, the number of flat bands will be $|N_A - N_B|$, [124] where N_A is the number of removed sites from sublattice A , and N_B the number of sites removed of sublattice B . In particular, this implies that generic bipartite lattices in which one site is removed will show a flat band. The Lieb lattice can be built by removing one site from the square lattice, leading to the existence of a flat band. In this very same fashion, other flat band models can be systematically constructed by removing a certain number of sites. These types of flat bands have been realized in artificial systems based on atomic lattices [127–131]. They can also be formed in suitable engineered, chemically synthesized lattices, where covalent organic frameworks and metal-organic frameworks are especially attractive systems for realizing these artificial models [132–140].

B. Experiments flat bands from frustration

There have been many theoretical proposals on metal-organic frameworks (MOFs) with kagome structure that should result in flat bands in their band structure [132, 133, 135]. However, the experimental demonstration has proven difficult. If the assembly is carried out directly on a metal substrate (typically Au(111), Ag(111) or Cu(111)), it is relatively straightforward to realize MOFs with a large degree of structural perfection [134]. Unfortunately, the relatively strong interaction with the underlying metal substrate typically masks the intrinsic electronic structure of the MOF. On the other hand, the formation of the high-quality MOFs on weakly interacting substrates is much more challenging [141, 142]

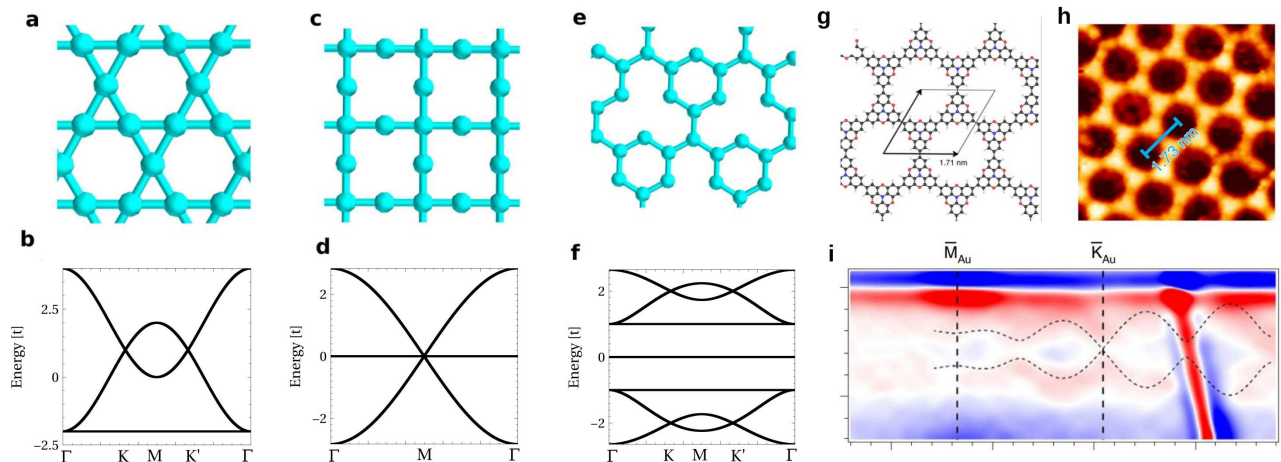


FIG. 5. Structure (a,c,e) and band structure (b,d,f) of different lattices featuring flat bands: the kagome lattice (a,b), the Lieb lattice (c,d) and a modified honeycomb lattice (e,f). (g,h) Schematic and experimental structure of a π -conjugated polymer poly-trioxazatriangulene [119]. (i) Second-derivative ARPES signal of the sample shown in panel h acquired at a photon energy of 120 eV. The dashed lines represent calculated bands for free-standing polymer network, shifted downwards by 0.12 eV [119].

and unambiguous proof of the flat bands has not been demonstrated.

The other chemical strategy for synthesizing two-dimensional networks on surfaces relies on the formation of covalent carbon-carbon bonds and structures called covalent organic frameworks (COFs). While there are extensive results on the formation of the one-dimensional nanocarbons (graphene nanoribbons) [131, 143–147], challenges remain to create two-dimensional assemblies with very high quality [148–150]. However, there are recent experimental results that are pushing this field towards higher quality samples towards the formation of flat bands in the MOF or COF band structure [119, 140, 142, 151]. The realized strategies rely on making a molecular network with a kagome lattice with one of the examples highlighted in Fig. 5g-i. In particular, on-surface polymerization was used to realize a high-quality two-dimensional polymer poly-trioxazatriangulene network [119]. This sample was of sufficiently high quality to allow angle-resolved photoemission spectroscopy (ARPES) experiments that can be used to directly probe the structure of the occupied bands as shown in Fig. 5i. This shows the folded bands of the valence band of the polymer that match the expected results well (calculated bands shown by dotted lines). The kagome flat band is expected to be at the bottom of the conduction band and cannot be directly probed by ARPES experiments. These results are along the path towards tuneable 2D organic or metal-organic structures with engineered flat bands. The incorporation of metal atoms with magnetism or a large spin-orbit interaction opens additional possibilities in realizing topological materials [132, 133, 152, 153].

C. Generating flat bands from long wavelength modulations

A simple way of generating nearly flat bands consists of weakly coupling quantum dot states. In this picture, the bandwidth is determined by the coupling between the quantum dots - the weaker it is, the flatter the resulting bands will be. A convenient way of achieving this in a real material in a large scale is by exploiting moiré patterns [154–160]. The fundamental idea relies on the locally modulated stacking over the moiré pattern that causes a spatial modulation of the conduction and valence band edges and leads the formation of a large scale array of quantum dots in twisted van der Waals superlattices. The mechanism for flat band generation can be rationalized from the decoupled limit, in which the system consists of decoupled quantum dots. The twist angle between the layers changes the size and separation between the quantum dots, promoting a finite hybridization between them that leads to nearly flat bands [159, 161, 162]. It is worth noting that this mechanism holds when there is a bandgap in the original materials (e.g. twisted h-BN and twisted dichalcogenide systems). This mechanism also requires the existence of a confinement gap. As a result, semimetals like graphene, in which electrons cannot be electrostatically confined, require a different mechanism for flat band generation. We will illustrate the use of gauge fields for this in section IV E.

D. Experiments flat bands from quantum dots

As we discussed above, flat bands can be realized in gapped, twisted moiré systems and this has been demonstrated in several experiments. An early experiment by

Zhang et al. relied on direct growth of rotationally aligned $\text{MoS}_2/\text{WSe}_2$ heterostructure, where the lattice mismatch then creates a moiré pattern [163]. While not directly resolving the flat bands spectroscopically, they demonstrated that the system had the necessary ingredients for their existence: the modulated interlayer coupling giving rise to a modulation of the conduction and valence band edge energies. They showed that the valence and conduction band edges are located at different layers and that the local bandgap was periodically modulated with an amplitude of ~ 0.15 eV, leading to the formation of a two-dimensional electronic superlattice.

The flat bands were directly identified in a later study [164], which concentrated on a twisted bilayer WSe_2 samples with twist angles of 3° and 57.5° . By using scanning tunnelling spectroscopy, it was possible to directly map the spatial extent of the wavefunctions at the flat-band energy and to show that the localization of the flat bands depends on the twist angle. The observed flat bands originated from the highest valence band at the Γ point (the conduction band onset varies very little over the moiré pattern and hence does not result in the type of quantum dot states required for the formation of the flat bands). The flat band in 3° twisted bilayer is localized on the hexagonal network separating the AA sites where as in the 57.5° systems, it is localized on the AB sites. These observations match well with the results of earlier atomic calculations [154].

While the basic physics of these systems can be understood with only considering the spatially varying stacking, in real materials, additional effects are expected to take place. For example, it is likely that there are some atomic-scale structural relaxations over the moiré pattern. This is precisely the effect that was assessed in the paper by Li et al. [165], who focussed on the twisted WSe_2/WS_2 system and used a combination of scanning tunneling spectroscopy (STS) experiments and *ab initio* simulations of TMD moiré superlattices. They find a strong 3D buckling reconstruction together with large in-plane strain redistribution in their heterostructures. Using STS imaging, they identify different types of flat bands originating either from the K -point at the valence band edge or from the Γ -point that gives rise to more deep-lying moiré flat bands. By analyzing the origin of these flat bands in detail, it is revealed that the K -point flat bands are mainly a result of the deformation of the monolayer. Similar behavior can be reproduced by considering only a puckered monolayer WSe_2 . On the other hand, the Γ -point flat bands are more in-line with the idea of the moiré induced, weakly coupled array of quantum dots. We will discuss the effects of periodic strain in more detail in section IV E.

The flat bands in the twisted TMD bilayers where the electron kinetic energy is suppressed are of course, fertile ground for realizing systems where interactions play a dominant role. There have been several publications on e.g. realizing different kinds of correlated states, correlated insulators and Wigner crystals in $\text{WSe}_2/\text{WSe}_2$ and

WSe_2/WS_2 moiré superlattices [166–168]. However, the moiré flat band systems can also have exciting optical effects and this has given birth to a field studying moiré excitons [169–172].

When the moiré period is larger than the exciton Bohr radius (around $\sim 1 - 2$ nm in e.g. MoSe_2 and WSe_2), the excitons will experience a spatially modulated periodic potential from the moiré. The other design parameter in heterobilayers is the relative alignment of the conduction and valence band edges, which allows the formation of intralayer excitons (e.g. WSe_2/WS_2 system where the electron and the hole reside in the same layer [171]), interlayer excitons (e.g. $\text{MoSe}_2/\text{WSe}_2$ system where the electron and the hole exist in different layers [169, 170]) and hybridized excitons (e.g. $\text{MoSe}_2/\text{WS}_2$ where the electron (for this system) is delocalized in the two layers [172]). Finally, the moiré-defined quantum dots preserve the three-fold rotational (C_3) symmetry, which implies that e.g. the interlayer excitons should inherit valley-contrasting properties [169]. These systems are currently under intense study to realize arrays of entangled quantum light emitters and realizing new exotic excitonic many-body phases (e.g. topological exciton insulator) [173, 174].

E. Generating flat bands from artificial gauge fields

A paradigmatic case of localized modes in a van der Waals material is non-uniform strained graphene (Fig. 6a). The appearance of flat bands in this system stems from the emergence of an artificial gauge field [57, 62, 178]. The effect of strain is to create a term in the system Hamiltonian that mimics a magnetic field (“pseudo-magnetic field”). However, this differs from a real magnetic field as the artificial gauge field manifests as a positive magnetic field for electrons in valley K and a negative electric field for electrons in valley K' , so that overall, the system does not break time-reversal symmetry.

The simplest instance of this is periodically rippled graphene monolayers [179–183] (Fig. 6b). The emergence of the gauge field can be easily rationalized from the graphene Hamiltonian [62]. For unstrained graphene, the low energy Hamiltonian in a single valley takes the form [184] $H = p_x \sigma_x + p_y \sigma_y$. In the presence of a global uniform strain, the Dirac point get displaced from the K and K' points, leading to Hamiltonian of the form $H = (p_x + A_x) \sigma_x + (p_y + A_y) \sigma_y$. Now, in a non-uniformly strained sample, we can take that there is a local strain that changes in real space, turning A_x and A_y spatially dependent. Noting that \vec{A} enters in the Dirac Hamiltonian as a canonical momentum, we can then identify a strain-induced artificial magnetic field as $\vec{B} = \nabla \times \vec{A}$.

Twisted graphene bilayers represent another case in which spatial modulations give rise to an artificial gauge field [57, 60]. In twisted graphene bilayers, the stacking in space changes between AA, AB and BA. The modulation

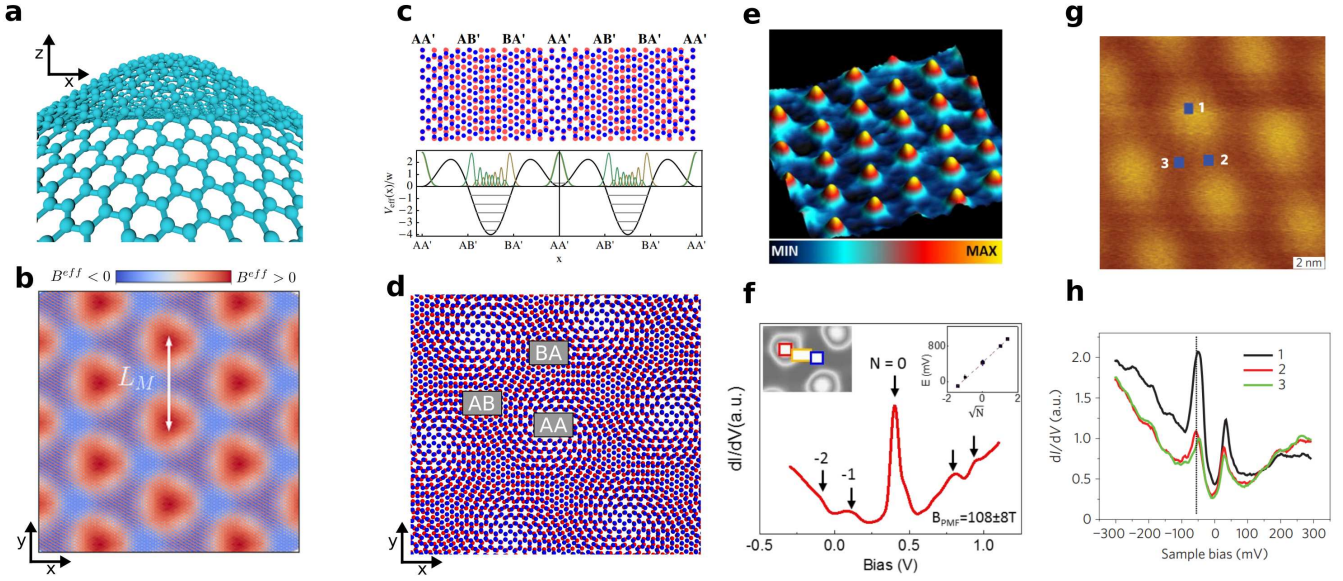


FIG. 6. Sketch of the buckling of a graphene monolayer (a) and spatial profile of the induced gauge field (b) [175]. Change in the local structure of a graphene bilayer leading to a non-abelian gauge field (c) [57], and profile of the moire unit cell (d). Panels (e,f) shows the topography (e) and dI/dV (f) of buckled graphene monolayer, showing the emergence of pseudo Landau levels.[176] Panel (f,g) shows the real-space STS (f) and dI/dV (g) of a twisted graphene bilayer at 1.8° , showing the emergence of van Hove singularities associated to non-abelian Landau levels.[177]

of the interlayer hopping due to the stacking brings up localized modes stemming from gauge fields, that can be rationalized as follows. A local Hamiltonian for a bilayer can be represented by a 4×4 Hamiltonian, in which the off-diagonal blocks contain the coupling between the two layers. Due to the modulated stacking (Fig. 6cd) the 2×2 interlayer coupling is modulated in space. Given the Dirac nature of the monolayer dispersion, that modulated hopping can be rationalized as an off-diagonal 2×2 gauge field, namely a non-abelian $SU(2)$ gauge field[57]. This non-abelian gauge field will thus give rise to associated pseudo Landau levels, the lowest one of them being the magic-angle flat bands at 1° [55, 56, 60].

F. Experiments flat bands from gauge fields

The earliest experiments showing the emergence of pseudo-Landau levels appeared in non-uniform strained graphene, which naturally appear in graphene nanobubbles[185]. In these setups van Hove singularities in the density of states were shown to appear, in contrast with the semimetallic spectra of unstrained samples. The emergence of those resonances is associated to the emergent gauge field, which was shown to correspond to up to an effective field of 300 T[185]. These nanobubbles can also be realized with graphene deposited on a weakly interacting substrate, and in that case, the STM tip could be used to tune the strain and hence, the pseudo-magnetic field [186, 187]. Finally, suspended graphene drumheads have also been used to investigate

the effects of pseudomagnetic fields and how they can confine the charge carriers in graphene [188, 189].

The buckling of graphene monolayers can also be created by choosing an appropriate substrate. In particular, recent experiments of graphene on top of $NbSe_2$ showed that graphene gets a spontaneous buckling on this structure. Associated to the buckling, a periodic non-uniform strain appears in the graphene monolayer, which gives rise to an elastic gauge field spontaneously[180, 182, 190]. Signatures of pseudo-Landau levels in this spontaneously buckled structure have been recently observed with STM[176].

The second example of pseudo-Landau levels corresponds to twisted bilayer graphene. Signatures of the lowest pseudo-Landau level, usually known as magic angle flat bands we observed early on, including some signature of symmetry breaking[177, 191, 192]. In particular, these pseudo-Landau-levels show a strong localization at the AA stacking regions of the twisted bilayer[177]. Interestingly, higher index Landau levels can also lead to correlated states[193], show different localization in the moire unit cell, and in particular the next van Hove singularity shows a higher extension around the AA regions[177, 191, 192]. Subsequent experiments have further explored the nature of the lowest flat band, in particular, observing spontaneous rotational symmetry breaking due to electronic interactions[194].

V. OUTLOOK

The possibility of artificial engineering states of matter with van der Waals materials has demonstrated a huge potential in the last few years. Beyond the instances of topological insulators and superconductors, quantum spin-liquids and flat band physics, their tunability opens prospects potentially opening radical new directions in quantum matter.

Starting with topological superconductors, a challenge for future experiments will be to braid the emergent Majorana modes, in an analogous way as it has been proposed for semiconductor nanowires[17, 18]. The possibility of switching on and off topological superconductivity with local gates provides a direction for extending these schemes to two-dimensional materials. Furthermore, artificial engineering can also allow engineering higher-order topological superconductors, in which the braiding of corner modes[195, 196] can open up a potential new direction for topological quantum computing with van der Waals materials.

Quantum spin-liquids open up exciting new experimental possibilities well beyond their experimental confirmation. First, the emergence of fractional spinon excitations in these systems opens possibilities to controllable spinon transport, and ultimately its interface with current spintronic devices[197, 198]. Secondly, the emergence of anyonic excitations in certain quantum spin liquids[199, 200] motivate potential future application of these systems for topological quantum computing[200].

Flat band systems further offer novel possibilities for emergent quantum matter, going beyond the well-known possibilities for high-temperature superconductivity and symmetry broken states. In particular, the emergence

of topologically non-trivial flat bands in twisted van der Waals materials provides an ideal starting point for fractional quantum Hall states in the absence of magnetic field, known as fractional Chern insulators[66, 201–204]. Analogous phenomenology for flat bands hosting spin-textured bands would further provide playgrounds for fractional quantum spin Hall physics, a state not found in nature yet. Ultimately, the combination of potential fractional quantum Hall physics and superconductivity in twisted multilayers provides an ideal starting point for engineering novel parafermion states[205, 206]. These states have resisted experimental realization so far due to the difficulty of having simultaneously fractional quantum Hall physics and superconductivity due to the large magnetic fields required. Such limitation would, however, not exist for intrinsic fractional quantum Hall states in graphene multilayers, providing an ideal solid state platform for parafermion physics.

Advances in the last few years have drastically proved the versatility of artificial engineering in van der Waals materials, revealing a variety of exotic phenomena previously only observed in rare compounds. While many of those proposals require further materials engineering and to further understand the physics of the underlying materials, the steady development of the field suggest that some of those goals may be achieved in the near future.

ACKNOWLEDGMENTS

We thank our group members - past and present - and colleagues for inspiration and insightful discussions. We acknowledge support from the European Research Council (ERC-2017-AdG no. 788185 “Artificial Designer Materials”) and Academy of Finland (Academy professor funding no. 318995 and Academy research fellow no. 331342).

-
- [1] Xiao-Liang Qi and Shou-Cheng Zhang, “Topological insulators and superconductors,” *Rev. Mod. Phys.* **83**, 1057–1110 (2011).
 - [2] M. Z. Hasan and C. L. Kane, “Colloquium: Topological insulators,” *Rev. Mod. Phys.* **82**, 3045–3067 (2010).
 - [3] Yoichi Ando, “Topological insulator materials,” *J. Phys. Soc. Jpn.* **82**, 102001 (2013).
 - [4] Chao-Xing Liu, Shou-Cheng Zhang, and Xiao-Liang Qi, “The quantum anomalous Hall effect: Theory and experiment,” *Annu. Rev. Condens. Matter Phys.* **7**, 301–321 (2016).
 - [5] Jason Alicea, “New directions in the pursuit of Majorana fermions in solid state systems,” *Rep. Prog. Phys.* **75**, 076501 (2012).
 - [6] Shawulien Kezilebieke, Md Nurul Huda, Viliam Vaňo, Markus Aapro, Somesh C. Ganguli, Orlando J. Silveira, Szczepan Głodzik, Adam S. Foster, Teemu Ojanen, and Peter Liljeroth, “Topological superconductivity in a van der Waals heterostructure,” *Nature* **588**, 424–428 (2020).
 - [7] A Yu Kitaev, “Unpaired majorana fermions in quantum wires,” *Physics-Uspeski* **44**, 131–136 (2001).
 - [8] Roman M. Lutchyn, Jay D. Sau, and S. Das Sarma, “Majorana fermions and a topological phase transition in semiconductor-superconductor heterostructures,” *Phys. Rev. Lett.* **105**, 077001 (2010).
 - [9] Yuval Oreg, Gil Refael, and Felix von Oppen, “Helical liquids and Majorana bound states in quantum wires,” *Phys. Rev. Lett.* **105**, 177002 (2010).
 - [10] Liang Fu and C. L. Kane, “Superconducting proximity effect and Majorana fermions at the surface of a topological insulator,” *Phys. Rev. Lett.* **100**, 096407 (2008).
 - [11] Liang Fu and C. L. Kane, “Josephson current and noise at a superconductor/quantum-spin-hall-insulator/superconductor junction,” *Phys. Rev. B* **79**, 161408 (2009).
 - [12] C.W.J. Beenakker, “Search for Majorana fermions in superconductors,” *Annu. Rev. Condens. Matter Phys.* **4**, 113–136 (2013).
 - [13] A. K. Geim and I. V. Grigorieva, “Van der Waals het-

- erostuctures,” *Nature* **499**, 419–425 (2013).
- [14] Miguel M. Ugeda, Aaron J. Bradley, Yi Zhang, Seita Onishi, Yi Chen, Wei Ruan, Claudia Ojeda-Aristizabal, Hyejin Ryu, Mark T. Edmonds, Hsin-Zon Tsai, Alexander Riss, Sung-Kwan Mo, Dunghai Lee, Alex Zettl, Zahid Hussain, Zhi-Xun Shen, and Michael F. Crommie, “Characterization of collective ground states in single-layer NbSe₂,” *Nat. Phys.* **12**, 92–97 (2015).
- [15] Bevin Huang, Genevieve Clark, Efrén Navarro-Moratalla, Dahlia R. Klein, Ran Cheng, Kyle L. Seyler, Ding Zhong, Emma Schmidgall, Michael A. McGuire, David H. Cobden, Wang Yao, Di Xiao, Pablo Jarillo-Herrero, and Xiaodong Xu, “Layer-dependent ferromagnetism in a van der Waals crystal down to the monolayer limit,” *Nature* **546**, 270–273 (2017).
- [16] M. Gibertini, M. Koperski, A. F. Morpurgo, and K. S. Novoselov, “Magnetic 2D materials and heterostructures,” *Nat. Nanotechnol.* **14**, 408–419 (2019).
- [17] Jason Alicea, Yuval Oreg, Gil Refael, Felix von Oppen, and Matthew P. A. Fisher, “Non-Abelian statistics and topological quantum information processing in 1D wire networks,” *Nat. Phys.* **7**, 412–417 (2011).
- [18] David Aasen, Michael Hell, Ryan V. Mishmash, Andrew Higginbotham, Jeroen Danon, Martin Leijnse, Thomas S. Jespersen, Joshua A. Folk, Charles M. Marcus, Karsten Flensberg, and Jason Alicea, “Milestones toward Majorana-based quantum computing,” *Phys. Rev. X* **6**, 031016 (2016).
- [19] S. M. Frolov, M. J. Manfra, and J. D. Sau, “Topological superconductivity in hybrid devices,” *Nat. Phys.* **16**, 718–724 (2020).
- [20] Manfred Sigrist and Kazuo Ueda, “Phenomenological theory of unconventional superconductivity,” *Rev. Mod. Phys.* **63**, 239–311 (1991).
- [21] V. Mourik, K. Zuo, S. M. Frolov, S. R. Plissard, E. P. A. M. Bakkers, and L. P. Kouwenhoven, “Signatures of Majorana fermions in hybrid superconductor-semiconductor nanowire devices,” *Science* **336**, 1003–1007 (2012).
- [22] R. M. Lutchyn, E. P. A. M. Bakkers, L. P. Kouwenhoven, P. Krogstrup, C. M. Marcus, and Y. Oreg, “Majorana zero modes in superconductor–semiconductor heterostructures,” *Nat. Rev. Mater.* **3**, 52–68 (2018).
- [23] Jelena Klinovaja, Peter Stano, Ali Yazdani, and Daniel Loss, “Topological superconductivity and majorana fermions in RKKY systems,” *Phys. Rev. Lett.* **111**, 186805 (2013).
- [24] S. Nadj-Perge, I. K. Drozdov, J. Li, H. Chen, S. Jeon, J. Seo, A. H. MacDonald, B. A. Bernevig, and A. Yazdani, “Observation of Majorana fermions in ferromagnetic atomic chains on a superconductor,” *Science* **346**, 602–607 (2014).
- [25] Benjamin E. Feldman, Mallika T. Randeria, Jian Li, Sangjun Jeon, Yonglong Xie, Zhijun Wang, Ilya K. Drozdov, B. Andrei Bernevig, and Ali Yazdani, “High-resolution studies of the Majorana atomic chain platform,” *Nat. Phys.* **13**, 286–291 (2016).
- [26] Michael Ruby, Benjamin W. Heinrich, Yang Peng, Felix von Oppen, and Katharina J. Franke, “Exploring a proximity-coupled Co chain on Pb(110) as a possible Majorana platform,” *Nano Lett.* **17**, 4473–4477 (2017).
- [27] Howon Kim, Alexandra Palacio-Morales, Thore Posske, Levente Rózsa, Krisztián Palotás, László Szunyogh, Michael Thorwart, and Roland Wiesendanger, “Toward tailoring Majorana bound states in artificially constructed magnetic atom chains on elemental superconductors,” *Sci. Adv.* **4**, eaar5251 (2018).
- [28] A. Kamlapure, L. Cornils, J. Wiebe, and R. Wiesendanger, “Engineering the spin couplings in atomically crafted spin chains on an elemental superconductor,” *Nat. Commun.* **9**, 3253 (2018).
- [29] Manuel Steinbrecher, Roman Rausch, Khai Ton That, Jan Hermenau, Alexander A. Khajetoorians, Michael Potthoff, Roland Wiesendanger, and Jens Wiebe, “Noncollinear spin states in bottom-up fabricated atomic chains,” *Nat. Commun.* **9**, 2853 (2018).
- [30] Lucas Schneider, Sascha Brinker, Manuel Steinbrecher, Jan Hermenau, Thore Posske, Manuel dos Santos Dias, Samir Lounis, Roland Wiesendanger, and Jens Wiebe, “Controlling in-gap end states by linking nonmagnetic atoms and artificially-constructed spin chains on superconductors,” *Nat. Commun.* **11**, 4707 (2020).
- [31] Hao-Hua Sun, Kai-Wen Zhang, Lun-Hui Hu, Chuang Li, Guan-Yong Wang, Hai-Yang Ma, Zhu-An Xu, Chun-Lei Gao, Dan-Dan Guan, Yao-Yi Li, Canhua Liu, Dong Qian, Yi Zhou, Liang Fu, Shao-Chun Li, Fu-Chun Zhang, and Jin-Feng Jia, “Majorana zero mode detected with spin selective Andreev reflection in the vortex of a topological superconductor,” *Phys. Rev. Lett.* **116**, 257003 (2016).
- [32] Alexandra Palacio-Morales, Eric Mascot, Sagen Cocklin, Howon Kim, Stephan Rachel, Dirk K. Morr, and Roland Wiesendanger, “Atomic-scale interface engineering of Majorana edge modes in a 2D magnet-superconductor hybrid system,” *Sci. Adv.* **5**, eaav6600 (2019).
- [33] Wenjin Zhao, Zaiyao Fei, Tiancheng Song, Han Kyou Choi, Tauno Palomaki, Bosong Sun, Paul Malinowski, Michael A. McGuire, Jiun-Haw Chu, Xiaodong Xu, and David H. Cobden, “Magnetic proximity and nonreciprocal current switching in a monolayer WTe₂ helical edge,” *Nat. Mater.* **19**, 503–507 (2020).
- [34] Yuan-Ming Lu and Ziqiang Wang, “Majorana fermions in spin-singlet nodal superconductors with coexisting noncollinear magnetic order,” *Phys. Rev. Lett.* **110**, 096403 (2013).
- [35] Rui-Xing Zhang, William S. Cole, and S. Das Sarma, “Helical hinge Majorana modes in iron-based superconductors,” *Phys. Rev. Lett.* **122**, 187001 (2019).
- [36] Zhenyu Wang, Jorge Olivares Rodriguez, Lin Jiao, Sean Howard, Martin Graham, G. D. Gu, Taylor L. Hughes, Dirk K. Morr, and Vidya Madhavan, “Evidence for dispersing 1D Majorana channels in an iron-based superconductor,” *Science* **367**, 104–108 (2020).
- [37] Dongfei Wang, Lingyuan Kong, Peng Fan, Hui Chen, Shiyu Zhu, Wenyao Liu, Lu Cao, Yujie Sun, Shixuan Du, John Schneeloch, Ruidan Zhong, Genda Gu, Liang Fu, Hong Ding, and Hong-Jun Gao, “Evidence for Majorana bound states in an iron-based superconductor,” *Science* **362**, 333–335 (2018).
- [38] Peng Zhang, Koichiro Yaji, Takahiro Hashimoto, Yuichi Ota, Takeshi Kondo, Kozo Okazaki, Zhijun Wang, Jinsheng Wen, G. D. Gu, Hong Ding, and Shik Shin, “Observation of topological superconductivity on the surface of an iron-based superconductor,” *Science* **360**, 182–186 (2018).
- [39] Shiyu Zhu, Lingyuan Kong, Lu Cao, Hui Chen, Michał Papaj, Shixuan Du, Yuqing Xing, Wenyao Liu, Dongfei

- Wang, Chengmin Shen, Fazhi Yang, John Schneeloch, Ruidan Zhong, Genda Gu, Liang Fu, Yu-Yang Zhang, Hong Ding, and Hong-Jun Gao, “Nearly quantized conductance plateau of vortex zero mode in an iron-based superconductor,” *Science* **367**, 189–192 (2019).
- [40] Qin Liu, Chen Chen, Tong Zhang, Rui Peng, Ya-Jun Yan, Chen-Hao-Ping Wen, Xia Lou, Yu-Long Huang, Jin-Peng Tian, Xiao-Li Dong, Guang-Wei Wang, Wei-Cheng Bao, Qiang-Hua Wang, Zhi-Ping Yin, Zhong-Xian Zhao, and Dong-Lai Feng, “Robust and clean Majorana zero mode in the vortex core of high-temperature superconductor $(\text{Li}_{0.84}\text{Fe}_{0.16})\text{OHFeSe}$,” *Phys. Rev. X* **8**, 041056 (2018).
- [41] Gerbold C. Ménard, Sébastien Guissart, Christophe Brun, Raphaël T. Leriche, Mircea Trif, François Debontridder, Dominique Demaille, Dimitri Roditchev, Pascal Simon, and Tristan Cren, “Two-dimensional topological superconductivity in $\text{Pb}/\text{Co}/\text{Si}(111)$,” *Nat. Commun.* **8**, 2040 (2017).
- [42] Shanshan Liu, Xiang Yuan, Yichao Zou, Yu Sheng, Ce Huang, Enze Zhang, Jiwei Ling, Yanwen Liu, Weiyi Wang, Cheng Zhang, Jin Zou, Kaiyou Wang, and Faxian Xiu, “Wafer-scale two-dimensional ferromagnetic Fe_3GeTe_2 thin films grown by molecular beam epitaxy,” *npj 2D Mater. Appl.* **1**, 30 (2017).
- [43] Weijong Chen, Zeyuan Sun, Zhongjie Wang, Lehua Gu, Xiaodong Xu, Shiwei Wu, and Chunlei Gao, “Direct observation of van der Waals stacking-dependent interlayer magnetism,” *Science* **366**, 983–987 (2019).
- [44] Shawulien Kezilebieke, Orlando J. Silveira, Md N. Huda, Viliam Vaňo, Markus Aapro, Somesh Chandra Ganguli, Jouko Lahtinen, Rhodri Mansell, Sebastiaan van Dijken, Adam S. Foster, and Peter Liljeroth, “Electronic and magnetic characterization of epitaxial CrBr_3 monolayers,” (2020), [arXiv:2009.13465 \[cond-mat.mtrl-sci\]](https://arxiv.org/abs/2009.13465).
- [45] Sergio C. de la Barrera, Michael R. Sinko, Devashish P. Gopalan, Nikhil Sivadas, Kyle L. Seyler, Kenji Watanabe, Takashi Taniguchi, Adam W. Tsen, Xiaodong Xu, Di Xiao, and Benjamin M. Hunt, “Tuning Ising superconductivity with layer and spin-orbit coupling in two-dimensional transition-metal dichalcogenides,” *Nat. Commun.* **9**, 1427 (2018).
- [46] Kun Zhao, Haicheng Lin, Xiao Xiao, Wantong Huang, Wei Yao, Mingzhe Yan, Ying Xing, Qinghua Zhang, Zi-Xiang Li, Shintaro Hoshino, Jian Wang, Shuyun Zhou, Lin Gu, Mohammad Saeed Bahramy, Hong Yao, Naoto Nagaosa, Qi-Kun Xue, Kam Tuen Law, Xi Chen, and Shuai-Hua Ji, “Disorder-induced multifractal superconductivity in monolayer niobium dichalcogenides,” *Nat. Phys.* **15**, 904–910 (2019).
- [47] Gerbold C. Ménard, Sébastien Guissart, Christophe Brun, Stéphane Pons, Vasily S. Stolyarov, François Debontridder, Matthieu V. Leclerc, Etienne Janod, Laurent Cario, Dimitri Roditchev, Pascal Simon, and Tristan Cren, “Coherent long-range magnetic bound states in a superconductor,” *Nat. Phys.* **11**, 1013–1016 (2015).
- [48] Ding Zhong, Kyle L. Seyler, Xiayu Linpeng, Nathan P. Wilson, Takashi Taniguchi, Kenji Watanabe, Michael A. McGuire, Kai-Mei C. Fu, Di Xiao, Wang Yao, and Xiaodong Xu, “Layer-resolved magnetic proximity effect in van der Waals heterostructures,” *Nat. Nanotechnol.* **15**, 187–191 (2020).
- [49] Livio Ciorciaro, Martin Kroner, Kenji Watanabe, Takashi Taniguchi, and Atac Imamoglu, “Observation of magnetic proximity effect using resonant optical spectroscopy of an electrically tunable $\text{MoSe}_2/\text{CrBr}_3$ heterostructure,” *Phys. Rev. Lett.* **124**, 197401 (2020).
- [50] Shawulien Kezilebieke, Viliam Vaňo, Md N. Huda, Markus Aapro, Somesh Chandra Ganguli, Peter Liljeroth, and Jose L. Lado, “Moiré-enabled topological superconductivity,” *arXiv e-prints*, arXiv:2011.09760 (2020), [arXiv:2011.09760 \[cond-mat.mes-hall\]](https://arxiv.org/abs/2011.09760).
- [51] L. Wang, I. Meric, P. Y. Huang, Q. Gao, Y. Gao, H. Tran, T. Taniguchi, K. Watanabe, L. M. Campos, D. A. Muller, J. Guo, P. Kim, J. Hone, K. L. Shepard, and C. R. Dean, “One-dimensional electrical contact to a two-dimensional material,” *Science* **342**, 614–617 (2013).
- [52] Yuan Cao, Valla Fatemi, Ahmet Demir, Shiang Fang, Spencer L. Tomarken, Jason Y. Luo, Javier D. Sanchez-Yamagishi, Kenji Watanabe, Takashi Taniguchi, Efthimios Kaxiras, Ray C. Ashoori, and Pablo Jarillo-Herrero, “Correlated insulator behaviour at half-filling in magic-angle graphene superlattices,” *Nature* **556**, 80–84 (2018).
- [53] M. Serlin, C. L. Tschirhart, H. Polshyn, Y. Zhang, J. Zhu, K. Watanabe, T. Taniguchi, L. Balents, and A. F. Young, “Intrinsic quantized anomalous Hall effect in a moiré heterostructure,” *Science* **367**, 900–903 (2019).
- [54] F. D. M. Haldane, “Model for a quantum Hall effect without Landau levels: Condensed-matter realization of the “parity anomaly,”” *Phys. Rev. Lett.* **61**, 2015–2018 (1988).
- [55] E. Suárez Morell, J. D. Correa, P. Vargas, M. Pacheco, and Z. Barticevic, “Flat bands in slightly twisted bilayer graphene: Tight-binding calculations,” *Phys. Rev. B* **82**, 121407 (2010).
- [56] R. Bistritzer and A. H. MacDonald, “Moiré bands in twisted double-layer graphene,” *Proceedings of the National Academy of Sciences* **108**, 12233–12237 (2011).
- [57] P. San-Jose, J. González, and F. Guinea, “Non-abelian gauge potentials in graphene bilayers,” *Phys. Rev. Lett.* **108**, 216802 (2012).
- [58] J. M. B. Lopes dos Santos, N. M. R. Peres, and A. H. Castro Neto, “Graphene bilayer with a twist: Electronic structure,” *Phys. Rev. Lett.* **99**, 256802 (2007).
- [59] Mikito Koshino, Noah F. Q. Yuan, Takashi Koretsune, Masayuki Ochi, Kazuhiko Kuroki, and Liang Fu, “Maximally localized Wannier orbitals and the extended Hubbard model for twisted bilayer graphene,” *Phys. Rev. X* **8**, 031087 (2018).
- [60] Jianpeng Liu, Junwei Liu, and Xi Dai, “Pseudo Landau level representation of twisted bilayer graphene: Band topology and implications on the correlated insulating phase,” *Phys. Rev. B* **99**, 155415 (2019).
- [61] D. J. Thouless, M. Kohmoto, M. P. Nightingale, and M. den Nijs, “Quantized Hall conductance in a two-dimensional periodic potential,” *Phys. Rev. Lett.* **49**, 405–408 (1982).
- [62] M.A.H. Vozmediano, M.I. Katsnelson, and F. Guinea, “Gauge fields in graphene,” *Physics Reports* **496**, 109–148 (2010).
- [63] Ya-Hui Zhang, Dan Mao, and T. Senthil, “Twisted bilayer graphene aligned with hexagonal boron nitride: Anomalous hall effect and a lattice model,” *Phys. Rev.*

- Research 1, 033126 (2019).**
- [64] Nick Bultinck, Shubhayu Chatterjee, and Michael P. Zaletel, “Mechanism for anomalous hall ferromagnetism in twisted bilayer graphene,” *Phys. Rev. Lett.* **124**, 166601 (2020).
- [65] Aaron L. Sharpe, Eli J. Fox, Arthur W. Barnard, Joe Finney, Kenji Watanabe, Takashi Taniguchi, M. A. Kastner, and David Goldhaber-Gordon, “Emergent ferromagnetism near three-quarters filling in twisted bilayer graphene,” *Science* **365**, 605–608 (2019).
- [66] Ahmed Abouelkomsan, Zhao Liu, and Emil J. Bergholtz, “Particle-hole duality, emergent Fermi liquids, and fractional Chern insulators in moiré flatbands,” *Phys. Rev. Lett.* **124**, 106803 (2020).
- [67] Kyoungwan Kim, Matthew Yankowitz, Babak Fallahazad, Sangwoo Kang, Hema C. P. Movva, Shengqiang Huang, Stefano Larentis, Chris M. Corbet, Takashi Taniguchi, Kenji Watanabe, Sanjay K. Banerjee, Brian J. LeRoy, and Emanuel Tutuc, “van der Waals heterostructures with high accuracy rotational alignment,” *Nano Lett.* **16**, 1989–1995 (2016).
- [68] Yuan Cao, Valla Fatemi, Shiang Fang, Kenji Watanabe, Takashi Taniguchi, Efthimios Kaxiras, and Pablo Jarillo-Herrero, “Unconventional superconductivity in magic-angle graphene superlattices,” *Nature* **556**, 43–50 (2018).
- [69] Kevin P. Nuckolls, Myungchul Oh, Dillon Wong, Biao Lian, Kenji Watanabe, Takashi Taniguchi, B. Andrei Bernevig, and Ali Yazdani, “Strongly correlated Chern insulators in magic-angle twisted bilayer graphene,” *Nature* **588**, 610–615 (2020).
- [70] Guorui Chen, Aaron L. Sharpe, Eli J. Fox, Ya-Hui Zhang, Shaoxin Wang, Lili Jiang, Bosai Lyu, Hongyuan Li, Kenji Watanabe, Takashi Taniguchi, Zhiwen Shi, T. Senthil, David Goldhaber-Gordon, Yuanbo Zhang, and Feng Wang, “Tunable correlated Chern insulator and ferromagnetism in a moiré superlattice,” *Nature* **579**, 56–61 (2020).
- [71] H. Polshyn, J. Zhu, M. A. Kumar, Y. Zhang, F. Yang, C. L. Tschirhart, M. Serlin, K. Watanabe, T. Taniguchi, A. H. MacDonald, and A. F. Young, “Electrical switching of magnetic order in an orbital Chern insulator,” *Nature* **588**, 66–70 (2020).
- [72] Shaowen Chen, Minhao He, Ya-Hui Zhang, Valerie Hsieh, Zaiyao Fei, K. Watanabe, T. Taniguchi, David H. Cobden, Xiaodong Xu, Cory R. Dean, and Matthew Yankowitz, “Electrically tunable correlated and topological states in twisted monolayer-bilayer graphene,” *Nat. Phys.* (2020), 10.1038/s41567-020-01062-6.
- [73] Shuang Wu, Zhenyuan Zhang, K. Watanabe, T. Taniguchi, and Eva Y. Andrei, “Chern insulators, van Hove singularities and topological flat bands in magic-angle twisted bilayer graphene,” *Nat. Mater.* (2021), 10.1038/s41563-020-00911-2.
- [74] Heung-Sik Kim, Vijay Shankar V., Andrei Catuneanu, and Hae-Young Kee, “Kitaev magnetism in honeycomb RuCl_3 with intermediate spin-orbit coupling,” *Phys. Rev. B* **91**, 241110 (2015).
- [75] Sananda Biswas, Ying Li, Stephen M. Winter, Johannes Knolle, and Roser Valentí, “Electronic properties of α - RuCl_3 in proximity to graphene,” *Phys. Rev. Lett.* **123**, 237201 (2019).
- [76] Eli Gerber, Yuan Yao, Tomas A. Arias, and Eun-Ah Kim, “Ab initio mismatched interface theory of graphene on α - RuCl_3 : Doping and magnetism,” *Phys. Rev. Lett.* **124**, 106804 (2020).
- [77] Y. Kasahara, T. Ohnishi, Y. Mizukami, O. Tanaka, Sixiao Ma, K. Sugii, N. Kurita, H. Tanaka, J. Nasu, Y. Motome, T. Shibauchi, and Y. Matsuda, “Majorana quantization and half-integer thermal quantum hall effect in a Kitaev spin liquid,” *Nature* **559**, 227–231 (2018).
- [78] P.W. Anderson, “Resonating valence bonds: A new kind of insulator?” *Materials Research Bulletin* **8**, 153–160 (1973).
- [79] Lucile Savary and Leon Balents, “Quantum spin liquids: a review,” *Rep. Prog. Phys.* **80**, 016502 (2016).
- [80] P. W. Anderson, “The resonating valence bond state in La_2CuO_4 and superconductivity,” *Science* **235**, 1196–1198 (1987).
- [81] G. Baskaran, Z. Zou, and P.W. Anderson, “The resonating valence bond state and high- T_c superconductivity — a mean field theory,” *Solid State Communications* **63**, 973–976 (1987).
- [82] Franz J. Wegner, “Duality in generalized ising models and phase transitions without local order parameters,” *Journal of Mathematical Physics* **12**, 2259–2272 (1971).
- [83] John B. Kogut, “An introduction to lattice gauge theory and spin systems,” *Rev. Mod. Phys.* **51**, 659–713 (1979).
- [84] Eduardo Fradkin, “Jordan-wigner transformation for quantum-spin systems in two dimensions and fractional statistics,” *Phys. Rev. Lett.* **63**, 322–325 (1989).
- [85] Alexei Kitaev, “Anyons in an exactly solved model and beyond,” *Annals of Physics* **321**, 2–111 (2006).
- [86] Xiao-Gang Wen, “Quantum orders in an exact soluble model,” *Phys. Rev. Lett.* **90**, 016803 (2003).
- [87] Jiří Chaloupka, George Jackeli, and Giniyat Khaliullin, “Kitaev-Heisenberg model on a honeycomb lattice: Possible exotic phases in iridium oxides A_2IrO_3 ,” *Phys. Rev. Lett.* **105**, 027204 (2010).
- [88] Yogesh Singh, S. Manni, J. Reuther, T. Berlijn, R. Thomale, W. Ku, S. Trebst, and P. Gegenwart, “Relevance of the Heisenberg-Kitaev model for the honeycomb lattice iridates A_2IrO_3 ,” *Phys. Rev. Lett.* **108**, 127203 (2012).
- [89] A. Banerjee, C. A. Bridges, J.-Q. Yan, A. A. Aczel, L. Li, M. B. Stone, G. E. Granroth, M. D. Lumsden, Y. Yiu, J. Knolle, S. Bhattacharjee, D. L. Kovrizhin, R. Moessner, D. A. Tennant, D. G. Mandrus, and S. E. Nagler, “Proximate Kitaev quantum spin liquid behaviour in a honeycomb magnet,” *Nat. Mater.* **15**, 733–740 (2016).
- [90] M. Hermanns, I. Kimchi, and J. Knolle, “Physics of the Kitaev model: Fractionalization, dynamic correlations, and material connections,” *Annu. Rev. Condens. Matter Phys.* **9**, 17–33 (2018).
- [91] S.-H. Baek, S.-H. Do, K.-Y. Choi, Y. S. Kwon, A. U. B. Wolter, S. Nishimoto, Jeroen van den Brink, and B. Büchner, “Evidence for a field-induced quantum spin liquid in α - RuCl_3 ,” *Phys. Rev. Lett.* **119**, 037201 (2017).
- [92] Arnab Banerjee, Jiaqiang Yan, Johannes Knolle, Craig A. Bridges, Matthew B. Stone, Mark D. Lumsden, David G. Mandrus, David A. Tennant, Roderich Moessner, and Stephen E. Nagler, “Neutron scattering in the proximate quantum spin liquid α - RuCl_3 ,” *Science* **356**, 1055–1059 (2017).
- [93] Seung-Hwan Do, Sang-Youn Park, Junki Yoshitake, Joji Nasu, Yukitoshi Motome, Yong Seung Kwon, D. T. Adroja, D. J. Voneshen, Kyoo Kim, T.-H. Jang, J.-H.

- Park, Kwang-Yong Choi, and Sungdae Ji, “Majorana fermions in the Kitaev quantum spin system α -RuCl₃,” *Nat. Phys.* **13**, 1079–1084 (2017).
- [94] Stephen M. Winter, Ying Li, Harald O. Jeschke, and Roser Valentí, “Challenges in design of Kitaev materials: Magnetic interactions from competing energy scales,” *Phys. Rev. B* **93**, 214431 (2016).
- [95] Stephen M. Winter, Kira Riedl, David Kaib, Radu Coldea, and Roser Valentí, “Probing α -rucl₃ beyond magnetic order: Effects of temperature and magnetic field,” *Phys. Rev. Lett.* **120**, 077203 (2018).
- [96] Stephen M. Winter, Kira Riedl, Pavel A. Maksimov, Alexander L. Chernyshev, Andreas Honecker, and Roser Valentí, “Breakdown of magnons in a strongly spin-orbital coupled magnet,” *Nat. Commun.* **8**, 1152 (2017).
- [97] Shuang Qiao, Xintong Li, Naizhou Wang, Wei Ruan, Cun Ye, Peng Cai, Zhenqi Hao, Hong Yao, Xianhui Chen, Jian Wu, Yayu Wang, and Zheng Liu, “Mottness collapse in 1T-TaS_{2-x}Se_x transition-metal dichalcogenide: An interplay between localized and itinerant orbitals,” *Phys. Rev. X* **7**, 041054 (2017).
- [98] K. Rossnagel and N. V. Smith, “Spin-orbit coupling in the band structure of reconstructed 1T-TaS₂,” *Phys. Rev. B* **73**, 073106 (2006).
- [99] Yi Chen, Wei Ruan, Meng Wu, Shujie Tang, Hyejin Ryu, Hsin-Zon Tsai, Ryan Lee, Salman Kahn, Franklin Liou, Caihong Jia, Oliver R. Albertini, Hongyu Xiong, Tao Jia, Zhi Liu, Jonathan A. Sobota, Amy Y. Liu, Joel E. Moore, Zhi-Xun Shen, Steven G. Louie, Sung-Kwan Mo, and Michael F. Crommie, “Strong correlations and orbital texture in single-layer 1T-TaSe₂,” *Nat. Phys.* **16**, 218–224 (2020).
- [100] Martin Klanjšek, Andrej Zorko, Rok Žitko, Jernej Mravlje, Zvonko Jagličić, Pabitra Kumar Biswas, Peter Prelovšek, Dragan Mihailovic, and Denis Arčon, “A high-temperature quantum spin liquid with polaron spins,” *Nature Physics* **13**, 1130–1134 (2017).
- [101] Timo Hyart, Anthony R. Wright, Giniyat Khaliullin, and Bernd Rosenow, “Competition between d -wave and topological p -wave superconducting phases in the doped Kitaev-Heisenberg model,” *Phys. Rev. B* **85**, 140510 (2012).
- [102] Soudabeh Mashhadi, Youngwook Kim, Jeongwoo Kim, Daniel Weber, Takashi Taniguchi, Kenji Watanabe, Noejung Park, Bettina Lotsch, Jurgen H. Smet, Marko Burghard, and Klaus Kern, “Spin-split band hybridization in graphene proximitized with α -RuCl₃ nanosheets,” *Nano Lett.* **19**, 4659–4665 (2019).
- [103] Boyi Zhou, J. Balgley, P. Lampen-Kelley, J.-Q. Yan, D. G. Mandrus, and E. A. Henriksen, “Evidence for charge transfer and proximate magnetism in graphene- α -rucl₃ heterostructures,” *Phys. Rev. B* **100**, 165426 (2019).
- [104] S. Yan, D. A. Huse, and S. R. White, “Spin-liquid ground state of the $s = 1/2$ kagome heisenberg antiferromagnet,” *Science* **332**, 1173–1176 (2011).
- [105] Tian-Heng Han, Joel S. Helton, Shaoyan Chu, Daniel G. Nocera, Jose A. Rodriguez-Rivera, Collin Broholm, and Young S. Lee, “Fractionalized excitations in the spin-liquid state of a kagome-lattice antiferromagnet,” *Nature* **492**, 406–410 (2012).
- [106] Stefan Depenbrock, Ian P. McCulloch, and Ulrich Schollwöck, “Nature of the spin-liquid ground state of the $s = 1/2$ heisenberg model on the kagome lattice,” *Phys. Rev. Lett.* **109**, 067201 (2012).
- [107] Subir Sachdev, “Kagome- and triangular-lattice Heisenberg antiferromagnets: Ordering from quantum fluctuations and quantum-disordered ground states with unconfined bosonic spinons,” *Phys. Rev. B* **45**, 12377–12396 (1992).
- [108] Luca Capriotti, Adolfo E. Trumper, and Sandro Sorella, “Long-range néel order in the triangular heisenberg model,” *Phys. Rev. Lett.* **82**, 3899–3902 (1999).
- [109] Steven R. White and A. L. Chernyshev, “Néel order in square and triangular lattice heisenberg models,” *Phys. Rev. Lett.* **99**, 127004 (2007).
- [110] Zhenyue Zhu, P. A. Maksimov, Steven R. White, and A. L. Chernyshev, “Topography of spin liquids on a triangular lattice,” *Phys. Rev. Lett.* **120**, 207203 (2018).
- [111] P. A. Maksimov, Zhenyue Zhu, Steven R. White, and A. L. Chernyshev, “Anisotropic-exchange magnets on a triangular lattice: Spin waves, accidental degeneracies, and dual spin liquids,” *Phys. Rev. X* **9**, 021017 (2019).
- [112] Shijie Hu, W. Zhu, Sebastian Eggert, and Yin-Chen He, “Dirac spin liquid on the spin-1/2 triangular heisenberg antiferromagnet,” *Phys. Rev. Lett.* **123**, 207203 (2019).
- [113] Samuel Mañas-Valero, Benjamin Huddart, Tom Lancaster, Eugenio Coronado, and Francis Pratt, “Quantum Phases and Spin Liquid Properties of 1T-TaS₂,” arXiv e-prints, arXiv:2007.15905 (2020), arXiv:2007.15905 [cond-mat.str-el].
- [114] Xian Liang Wu and Charles M. Lieber, “Hexagonal domain-like charge density wave phase of TaS₂ determined by scanning tunneling microscopy,” *Science* **243**, 1703–1705 (1989).
- [115] Xian Liang Wu and Charles M. Lieber, “Direct observation of growth and melting of the hexagonal-domain charge-density-wave phase in 1t-tas₂ by scanning tunneling microscopy,” *Phys. Rev. Lett.* **64**, 1150–1153 (1990).
- [116] Jae Whan Park, Gil Young Cho, Jinwon Lee, and Han Woong Yeom, “Emergent honeycomb network of topological excitations in correlated charge density wave,” *Nat. Commun.* **10**, 4038 (2019).
- [117] K. T. Law and Patrick A. Lee, “1T-TaS₂ as a quantum spin liquid,” *Proc. Acad. Nat. Sci.* **114**, 6996–7000 (2017).
- [118] Doohee Cho, Yong-Heum Cho, Sang-Wook Cheong, Ki-Seok Kim, and Han Woong Yeom, “Interplay of electron-electron and electron-phonon interactions in the low-temperature phase of 1T-TaS₂,” *Phys. Rev. B* **92**, 085132 (2015).
- [119] G. Galeotti, F. De Marchi, E. Hamzehpoor, O. MacLean, M. Rajeswara Rao, Y. Chen, L. V. Besteiro, D. Dettmann, L. Ferrari, F. Frezza, P. M. Sheverdyeva, R. Liu, A. K. Kundu, P. Moras, M. Ebrahimi, M. C. Gallagher, F. Rosei, D. F. Perepichka, and G. Contini, “Synthesis of mesoscale ordered two-dimensional π -conjugated polymers with semiconducting properties,” *Nat. Mater.* **19**, 874–880 (2020).
- [120] Elio J. König, Mallika T. Randeria, and Berthold Jäck, “Tunneling spectroscopy of quantum spin liquids,” *Phys. Rev. Lett.* **125**, 267206 (2020).
- [121] Wei Ruan, Yi Chen, Shujie Tang, Jinwoong Hwang, Hsin-Zon Tsai, Ryan Lee, Meng Wu, Hyejin Ryu, Salman Kahn, Franklin Liou, Caihong Jia, Andrew

- Aikawa, Choongyu Hwang, Feng Wang, Yongseong Choi, Steven G. Louie, Patrick A. Lee, Zhi-Xun Shen, Sung-Kwan Mo, and Michael F. Crommie, “Imaging spinon density modulations in a 2D quantum spin liquid,” (2020), [arXiv:2009.07379 \[cond-mat.str-el\]](https://arxiv.org/abs/2009.07379).
- [122] M. Gomilšek, R. Žitko, M. Klanjšek, M. Pregelj, C. Baines, Y. Li, Q. M. Zhang, and A. Zorko, “Kondo screening in a charge-insulating spinon metal,” *Nature Physics* **15**, 754–758 (2019).
- [123] Daniel Leykam, Alexei Andreanov, and Sergej Flach, “Artificial flat band systems: from lattice models to experiments,” *Adv. Phys.: X* **3**, 1473052 (2018).
- [124] Elliott H. Lieb, “Two theorems on the hubbard model,” *Phys. Rev. Lett.* **62**, 1201–1204 (1989).
- [125] N. B. Kopnin, T. T. Heikkilä, and G. E. Volovik, “High-temperature surface superconductivity in topological flat-band systems,” *Phys. Rev. B* **83**, 220503(R) (2011).
- [126] Doron L. Bergman, Congjun Wu, and Leon Balents, “Band touching from real-space topology in frustrated hopping models,” *Phys. Rev. B* **78**, 125104 (2008).
- [127] Robert Drost, Teemu Ojanen, Ari Harju, and Peter Liljeroth, “Topological states in engineered atomic lattices,” *Nat. Phys.* **13**, 668–671 (2017).
- [128] Marlou R. Slot, Thomas S. Gardenier, Peter H. Jacobse, Guido C. P. van Miert, Sander N. Kempkes, Stephan J. M. Zevenhuizen, Cristiane Morais Smith, Daniel Vanmaekelbergh, and Ingmar Swart, “Experimental realization and characterization of an electronic Lieb lattice,” *Nat. Phys.* **13**, 672–676 (2017).
- [129] Md Nurul Huda, Shawulienu Kezilebieke, and Peter Liljeroth, “Designer flat bands in quasi-one-dimensional atomic lattices,” *Phys. Rev. Research* **2**, 043426 (2020).
- [130] Alexander A. Khajetoorians, Daniel Wegner, Alexander F. Otte, and Ingmar Swart, “Creating designer quantum states of matter atom-by-atom,” *Nat. Rev. Phys.* **1**, 703–715 (2019).
- [131] Linghao Yan and Peter Liljeroth, “Engineered electronic states in atomically precise artificial lattices and graphene nanoribbons,” *Adv. Phys.: X* **4**, 1651672 (2019).
- [132] Z. F. Wang, Ninghai Su, and Feng Liu, “Prediction of a two-dimensional organic topological insulator,” *Nano Lett.* **13**, 2842–2845 (2013).
- [133] Z.F Wang, Zheng Liu, and Feng Liu, “Organic topological insulators in organometallic lattices,” *Nat. Commun.* **4** (2013), 10.1038/ncomms2451.
- [134] Lei Dong, Zi’Ang Gao, and Nian Lin, “Self-assembly of metal–organic coordination structures on surfaces,” *Prog. Surf. Sci.* **91**, 101–135 (2016).
- [135] L. Z. Zhang, Z. F. Wang, B. Huang, B. Cui, Zhiming Wang, S. X. Du, H.-J. Gao, and Feng Liu, “Intrinsic two-dimensional organic topological insulators in metal–dicyanoanthracene lattices,” *Nano Lett.* **16**, 2072–2075 (2016).
- [136] Liang Dong, Youngkuk Kim, Dequan Er, Andrew M. Rappe, and Vivek B. Shenoy, “Two-dimensional π -conjugated covalent-organic frameworks as quantum anomalous Hall topological insulators,” *Phys. Rev. Lett.* **116**, 096601 (2016).
- [137] Avijit Kumar, Kaustuv Banerjee, and Peter Liljeroth, “Molecular assembly on two-dimensional materials,” *Nanotechnology* **28**, 082001 (2017).
- [138] Hao Sun, Shijing Tan, Min Feng, Jin Zhao, and Hrvoje Petek, “Deconstruction of the electronic properties of a topological insulator with a two-dimensional noble metal–organic honeycomb–kagome band structure,” *J. Phys. Chem. C* **122**, 18659–18668 (2018).
- [139] Maximilian A. Springer, Tsai-Jung Liu, Agnieszka Kuc, and Thomas Heine, “Topological two-dimensional polymers,” *Chem. Soc. Rev.* **49**, 2007–2019 (2020).
- [140] Rémy Pawlak, Xunshan Liu, Silviya Ninova, Philipp D’astolfo, Carl Drechsel, Jung-Ching Liu, Robert Häner, Silvio Decurtins, Ulrich Aschauer, Shi-Xia Liu, and Ernst Meyer, “On-surface synthesis of nitrogen-doped kagome graphene,” *Angew. Chem. Int. Ed.* (2021), 10.1002/anie.202016469.
- [141] Avijit Kumar, Kaustuv Banerjee, Adam S. Foster, and Peter Liljeroth, “Two-dimensional band structure in honeycomb metal–organic frameworks,” *Nano Lett.* **18**, 5596–5602 (2018).
- [142] Linghao Yan, Orlando J. Silveira, Benjamin Alldritt, Ondřej Krejčí, Adam S. Foster, and Peter Liljeroth, “Synthesis and gating the charge state of a monolayer metal-organic framework,” (2020), [arXiv:2007.06899 \[cond-mat.mtrl-sci\]](https://arxiv.org/abs/2007.06899).
- [143] Jinming Cai, Pascal Ruffieux, Rached Jaafar, Marco Bieri, Thomas Braun, Stephan Blankenburg, Matthias Muoth, Ari P. Seitsonen, Moussa Saleh, Xinliang Feng, Klaus Müllen, and Roman Fasel, “Atomically precise bottom-up fabrication of graphene nanoribbons,” *Nature* **466**, 470–473 (2010).
- [144] Pascal Ruffieux, Shiyong Wang, Bo Yang, Carlos Sánchez-Sánchez, Jia Liu, Thomas Dienel, Leopold Talirz, Prashant Shinde, Carlo A. Pignedoli, Daniele Passerone, Tim Dumschlaff, Xinliang Feng, Klaus Müllen, and Roman Fasel, “On-surface synthesis of graphene nanoribbons with zigzag edge topology,” *Nature* **531**, 489–492 (2016).
- [145] Leopold Talirz, Pascal Ruffieux, and Roman Fasel, “On-surface synthesis of atomically precise graphene nanoribbons,” *Adv. Mater.* **28**, 6222–6231 (2016).
- [146] Oliver Gröning, Shiyong Wang, Xuelin Yao, Carlo A. Pignedoli, Gabriela Borin Barin, Colin Daniels, Andrew Cupo, Vincent Meunier, Xinliang Feng, Akimitsu Narita, Klaus Müllen, Pascal Ruffieux, and Roman Fasel, “Engineering of robust topological quantum phases in graphene nanoribbons,” *Nature* **560**, 209–213 (2018).
- [147] Daniel J. Rizzo, Gregory Veber, Ting Cao, Christopher Bronner, Ting Chen, Fangzhou Zhao, Henry Rodriguez, Steven G. Louie, Michael F. Crommie, and Felix R. Fischer, “Topological band engineering of graphene nanoribbons,” *Nature* **560**, 204–208 (2018).
- [148] Dimas G. de Oteyza and Celia Rogero, eds., *On-Surface Synthesis II* (Springer International Publishing, 2018).
- [149] Sylvain Clair and Dimas G. de Oteyza, “Controlling a chemical coupling reaction on a surface: Tools and strategies for on-surface synthesis,” *Chem. Rev.* **119**, 4717–4776 (2019).
- [150] Leonhard Grill and Stefan Hecht, “Covalent on-surface polymerization,” *Nat. Chem.* **12**, 115–130 (2020).
- [151] Daniel J. Rizzo, Qingqing Dai, Christopher Bronner, Gregory Veber, Brian J. Smith, Michio Matsumoto, Simil Thomas, Giang D. Nguyen, Patrick R. Forrester, William Zhao, Jakob H. Jørgensen, William R. Dichtel, Felix R. Fischer, Hong Li, Jean-Luc Bredas, and Michael F. Crommie, “Revealing the local electronic

- structure of a single-layer covalent organic framework through electronic decoupling,” *Nano Lett.* **20**, 963–970 (2020).
- [152] Linghao Yan, Bowen Xia, Qiushi Zhang, Guowen Kuang, Hu Xu, Jun Liu, Pei Nian Liu, and Nian Lin, “Stabilizing and organizing Bi_3Cu_4 and $\text{Bi}_7\text{Cu}_{12}$ nanoclusters in two-dimensional metal-organic networks,” *Angew. Chem. Int. Ed.* **57**, 4617–4621 (2018).
- [153] Zi’Ang Gao, Chia-Hsiu Hsu, Jing Liu, Feng-Chuan Chuang, Ran Zhang, Bowen Xia, Hu Xu, Li Huang, Qiao Jin, Pei Nian Liu, and Nian Lin, “Synthesis and characterization of a single-layer conjugated metal-organic structure featuring a non-trivial topological gap,” *Nanoscale* **11**, 878–881 (2019).
- [154] Mit H. Naik and Manish Jain, “Ultraflatbands and shear solitons in moiré patterns of twisted bilayer transition metal dichalcogenides,” *Phys. Rev. Lett.* **121**, 266401 (2018).
- [155] Narasimha Raju Chebrolu, Bheema Lingam Chittari, and Jeil Jung, “Flat bands in twisted double bilayer graphene,” *Phys. Rev. B* **99**, 235417 (2019).
- [156] V. V. Enaldiev, V. Zólyomi, C. Yelgel, S. J. Magorrian, and V. I. Fal’ko, “Stacking domains and dislocation networks in marginally twisted bilayers of transition metal dichalcogenides,” *Phys. Rev. Lett.* **124**, 206101 (2020).
- [157] Stephen Carr, Daniel Massatt, Steven B. Torrisi, Paul Cazeaux, Mitchell Luskin, and Efthimios Kaxiras, “Relaxation and domain formation in incommensurate two-dimensional heterostructures,” *Phys. Rev. B* **98**, 224102 (2018).
- [158] Astrid Weston, Yichao Zou, Vladimir Enaldiev, Alex Summerfield, Nicholas Clark, Viktor Zólyomi, Abigail Graham, Celal Yelgel, Samuel Magorrian, Mingwei Zhou, Johanna Zultak, David Hopkinson, Alexei Barinov, Thomas H. Bointon, Andrey Kretinin, Neil R. Wilson, Peter H. Beton, Vladimir I. Fal’ko, Sarah J. Haigh, and Roman Gorbachev, “Atomic reconstruction in twisted bilayers of transition metal dichalcogenides,” *Nat. Nanotechnol* **15**, 592–597 (2020).
- [159] Lede Xian, Dante M. Kennes, Nicolas Tancogne-Dejean, Massimo Altarelli, and Angel Rubio, “Multiflat bands and strong correlations in twisted bilayer boron nitride: Doping-induced correlated insulator and superconductor,” *Nano Letters* **19**, 4934–4940 (2019).
- [160] Mit H. Naik, Sudipta Kundu, Indrajit Maity, and Manish Jain, “Origin and evolution of ultraflat bands in twisted bilayer transition metal dichalcogenides: Realization of triangular quantum dots,” *Phys. Rev. B* **102**, 075413 (2020).
- [161] Yang Zhang, Tongtong Liu, and Liang Fu, “Electrically tunable charge transfer and charge orders in twisted transition metal dichalcogenide bilayers,” arXiv e-prints, arXiv:2009.14224 (2020), arXiv:2009.14224 [cond-mat.str-el].
- [162] M. Angeli and A. H. MacDonald, “ Γ -Valley Transition-Metal-Dichalcogenide Moiré Bands,” arXiv e-prints, arXiv:2008.01735 (2020), arXiv:2008.01735 [cond-mat.str-el].
- [163] Chendong Zhang, Chih-Piao Chuu, Xibiao Ren, Ming-Yang Li, Lain-Jong Li, Chuanhong Jin, Mei-Yin Chou, and Chih-Kang Shih, “Interlayer couplings, moiré patterns, and 2D electronic superlattices in $\text{MoS}_2/\text{WSe}_2$ hetero-bilayers,” *Sci. Adv.* **3**, e1601459 (2017).
- [164] Zhiming Zhang, Yimeng Wang, Kenji Watanabe, Takashi Taniguchi, Keiji Ueno, Emanuel Tutuc, and Brian J. LeRoy, “Flat bands in twisted bilayer transition metal dichalcogenides,” *Nat. Phys.* (2020), 10.1038/s41567-020-0958-x.
- [165] Hongyuan Li, Shaowei Li, Mit H. Naik, Jingxu Xie, Xinyu Li, Jiayin Wang, Emma Regan, Danqing Wang, Wenyu Zhao, Sihan Zhao, Salman Kahn, Kentaro Yumigeta, Mark Blei, Takashi Taniguchi, Kenji Watanabe, Sefaattin Tongay, Alex Zettl, Steven G. Louie, Feng Wang, and Michael F. Crommie, “Imaging moiré flat bands in three-dimensional reconstructed WSe_2/WS_2 superlattices,” *Nat. Mater.* (2021), 10.1038/s41563-021-00923-6.
- [166] Lei Wang, En-Min Shih, Augusto Ghiotto, Lede Xian, Daniel A. Rhodes, Cheng Tan, Martin Claassen, Dante M. Kennes, Yusong Bai, Bumho Kim, Kenji Watanabe, Takashi Taniguchi, Xiaoyang Zhu, James Hone, Angel Rubio, Abhay N. Pasupathy, and Cory R. Dean, “Correlated electronic phases in twisted bilayer transition metal dichalcogenides,” *Nat. Mater.* **19**, 861–866 (2020).
- [167] Yanhao Tang, Lizhong Li, Tingxin Li, Yang Xu, Song Liu, Katayun Barmak, Kenji Watanabe, Takashi Taniguchi, Allan H. MacDonald, Jie Shan, and Kin Fai Mak, “Simulation of Hubbard model physics in WSe_2/WS_2 moiré superlattices,” *Nature* **579**, 353–358 (2020).
- [168] Emma C. Regan, Danqing Wang, Chenhao Jin, M. Iqbal Bakti Utama, Beini Gao, Xin Wei, Sihan Zhao, Wenyu Zhao, Zuocheng Zhang, Kentaro Yumigeta, Mark Blei, Johan D. Carlström, Kenji Watanabe, Takashi Taniguchi, Sefaattin Tongay, Michael Crommie, Alex Zettl, and Feng Wang, “Mott and generalized wigner crystal states in WSe_2/WS_2 moiré superlattices,” *Nature* **579**, 359–363 (2020).
- [169] Kyle L. Seyler, Pasqual Rivera, Hongyi Yu, Nathan P. Wilson, Essance L. Ray, David G. Mandrus, Jiaqiang Yan, Wang Yao, and Xiaodong Xu, “Signatures of moiré-trapped valley excitons in $\text{MoSe}_2/\text{WSe}_2$ hetero-bilayers,” *Nature* **567**, 66–70 (2019).
- [170] Kha Tran, Galan Moody, Fengcheng Wu, Xiaobo Lu, Junho Choi, Kyoungwan Kim, Amritesh Rai, Daniel A. Sanchez, Jiamin Quan, Akshay Singh, Jacob Embley, André Zepeda, Marshall Campbell, Travis Autry, Takashi Taniguchi, Kenji Watanabe, Nanshu Lu, Sanjay K. Banerjee, Kevin L. Silverman, Suenne Kim, Emanuel Tutuc, Li Yang, Allan H. MacDonald, and Xiaojin Li, “Evidence for moiré excitons in van der Waals heterostructures,” *Nature* **567**, 71–75 (2019).
- [171] Chenhao Jin, Emma C. Regan, Aiming Yan, M. Iqbal Bakti Utama, Danqing Wang, Sihan Zhao, Ying Qin, Sijie Yang, Zhiren Zheng, Shenyang Shi, Kenji Watanabe, Takashi Taniguchi, Sefaattin Tongay, Alex Zettl, and Feng Wang, “Observation of moiré excitons in WSe_2/WS_2 heterostructure superlattices,” *Nature* **567**, 76–80 (2019).
- [172] Evgeny M. Alexeev, David A. Ruiz-Tijerina, Mark Danovich, Matthew J. Hamer, Daniel J. Terry, Pramoda K. Nayak, Seongjoon Ahn, Sangyeon Pak, Juwon Lee, Jung Inn Sohn, Maciej R. Molas, Maciej Koperski, Kenji Watanabe, Takashi Taniguchi, Kostya S. Novoselov, Roman V. Gorbachev, Hyeon Suk Shin, Vladimir I. Fal’ko, and Alexander I. Tartakovskii, “Resonantly hybridized excitons in moiré superlattices in van

- der Waals heterostructures,” *Nature* **567**, 81–86 (2019).
- [173] Zefang Wang, Daniel A. Rhodes, Kenji Watanabe, Takashi Taniguchi, James C. Hone, Jie Shan, and Kin Fai Mak, “Evidence of high-temperature exciton condensation in two-dimensional atomic double layers,” *Nature* **574**, 76–80 (2019).
- [174] Alexander Tartakovskii, “Excitons in 2D heterostructures,” *Nat. Rev. Phys.* **2**, 8–9 (2019).
- [175] A L R Manesco, J L Lado, E V S Ribeiro, G Weber, and D Rodrigues Jr, “Correlations in the elastic landau level of spontaneously buckled graphene,” *2D Materials* **8**, 015011 (2020).
- [176] Jinhai Mao, Slaviša P. Milovanović, Miša Anđelković, Xinyuan Lai, Yang Cao, Kenji Watanabe, Takashi Taniguchi, Lucian Covaci, Francois M. Peeters, Andre K. Geim, Yuhang Jiang, and Eva Y. Andrei, “Evidence of flat bands and correlated states in buckled graphene superlattices,” *Nature* **584**, 215–220 (2020).
- [177] Guohong Li, A. Luican, J. M. B. Lopes dos Santos, A. H. Castro Neto, A. Reina, J. Kong, and E. Y. Andrei, “Observation of Van Hove singularities in twisted graphene layers,” *Nat. Phys.* **6**, 109–113 (2009).
- [178] Aline Ramires and Jose L. Lado, “Electrically tunable gauge fields in tiny-angle twisted bilayer graphene,” *Phys. Rev. Lett.* **121**, 146801 (2018).
- [179] A. L. Vázquez de Parga, F. Calleja, B. Borca, M. C. G. Passeggi, J. J. Hinarejos, F. Guinea, and R. Miranda, “Periodically rippled graphene: Growth and spatially resolved electronic structure,” *Phys. Rev. Lett.* **100**, 056807 (2008).
- [180] F. Guinea, Baruch Horowitz, and P. Le Doussal, “Gauge fields, ripples and wrinkles in graphene layers,” *Solid State Communications* **149**, 1140–1143 (2009).
- [181] F. Guinea, M. I. Katsnelson, and A. K. Geim, “Energy gaps and a zero-field quantum hall effect in graphene by strain engineering,” *Nature Physics* **6**, 30–33 (2009).
- [182] M. Ramezani Masir, D. Moldovan, and F.M. Peeters, “Pseudo magnetic field in strained graphene: Revisited,” *Solid State Communications* **175–176**, 76–82 (2013).
- [183] B. Amorim, A. Cortijo, F. de Juan, A.G. Grushin, F. Guinea, A. Gutiérrez-Rubio, H. Ochoa, V. Parante, R. Roldán, P. San-Jose, J. Schiefele, M. Sturla, and M.A.H. Vozmediano, “Novel effects of strains in graphene and other two dimensional materials,” *Physics Reports* **617**, 1–54 (2016).
- [184] A. H. Castro Neto, F. Guinea, N. M. R. Peres, K. S. Novoselov, and A. K. Geim, “The electronic properties of graphene,” *Rev. Mod. Phys.* **81**, 109–162 (2009).
- [185] N. Levy, S. A. Burke, K. L. Meaker, M. Panlasigui, A. Zettl, F. Guinea, A. H. C. Neto, and M. F. Crommie, “Strain-induced pseudo-magnetic fields greater than 300 tesla in graphene nanobubbles,” *Science* **329**, 544–547 (2010).
- [186] T. Mashoff, M. Pratzler, V. Geringer, T. J. Echtermeyer, M. C. Lemme, M. Liebmann, and M. Morgenstern, “Bistability and oscillatory motion of natural nanomembranes appearing within monolayer graphene on silicon dioxide,” *Nano Lett.* **10**, 461–465 (2010).
- [187] Alexander Georgi, Peter Nemes-Incze, Ramon Carrillo-Bastos, Daiara Faria, Silvia Viola Kusminskiy, Dawei Zhai, Martin Schneider, Dinesh Subramaniam, Torge Mashoff, Nils M. Freitag, Marcus Liebmann, Marco Pratzler, Ludger Wirtz, Colin R. Woods, Roman V. Gorbachev, Yang Cao, Kostya S. Novoselov, Nancy Sandler, and Markus Morgenstern, “Tuning the pseudospin polarization of graphene by a pseudomagnetic field,” *Nano Lett.* **17**, 2240–2245 (2017).
- [188] N. N. Klimov, S. Jung, S. Zhu, T. Li, C. A. Wright, S. D. Solares, D. B. Newell, N. B. Zhitenev, and J. A. Stroschio, “Electromechanical properties of graphene drumheads,” *Science* **336**, 1557–1561 (2012).
- [189] Shuze Zhu, Yinjun Huang, Nikolai N. Klimov, David B. Newell, Nikolai B. Zhitenev, Joseph A. Stroschio, Santiago D. Solares, and Teng Li, “Pseudomagnetic fields in a locally strained graphene drumhead,” *Phys. Rev. B* **90**, 075426 (2014).
- [190] M. Schneider, D. Faria, S. Viola Kusminskiy, and N. Sandler, “Local sublattice symmetry breaking for graphene with a centrosymmetric deformation,” *Phys. Rev. B* **91**, 161407 (2015).
- [191] I. Brihuega, P. Mallet, H. González-Herrero, G. Trambly de Laissardière, M. M. Ugeda, L. Magaud, J. M. Gómez-Rodríguez, F. Ynduráin, and J.-Y. Veuillen, “Unraveling the intrinsic and robust nature of van hove singularities in twisted bilayer graphene by scanning tunneling microscopy and theoretical analysis,” *Phys. Rev. Lett.* **109**, 196802 (2012).
- [192] Dillon Wong, Yang Wang, Jeil Jung, Sergio Pezzini, Ashley M. DaSilva, Hsin-Zon Tsai, Han Sae Jung, Ramin Khajeh, Youngkyou Kim, Juwon Lee, Salman Kahn, Sajjad Tollabimazraehno, Haider Rasool, Kenji Watanabe, Takashi Taniguchi, Alex Zettl, Shaffique Adam, Allan H. MacDonald, and Michael F. Crommie, “Local spectroscopy of moiré-induced electronic structure in gate-tunable twisted bilayer graphene,” *Phys. Rev. B* **92**, 155409 (2015).
- [193] Emilio Codecido, Qiyue Wang, Ryan Koester, Shi Che, Haidong Tian, Rui Lv, Son Tran, Kenji Watanabe, Takashi Taniguchi, Fan Zhang, Marc Bockrath, and Chun Ning Lau, “Correlated insulating and superconducting states in twisted bilayer graphene below the magic angle,” *Sci. Adv.* **5**, eaaw9770 (2019).
- [194] Yuhang Jiang, Xinyuan Lai, Kenji Watanabe, Takashi Taniguchi, Kristjan Haule, Jinhai Mao, and Eva Y. Andrei, “Charge order and broken rotational symmetry in magic-angle twisted bilayer graphene,” *Nature* **573**, 91–95 (2019).
- [195] Tudor E. Pahomi, Manfred Sigrist, and Alexey A. Soluyanov, “Braiding majorana corner modes in a second-order topological superconductor,” *Phys. Rev. Research* **2**, 032068 (2020).
- [196] Song-Bo Zhang, W. B. Rui, Alessio Calzona, Sang-Jun Choi, Andreas P. Schnyder, and Björn Trauzettel, “Topological and holonomic quantum computation based on second-order topological superconductors,” *Phys. Rev. Research* **2**, 043025 (2020).
- [197] A. Avsar, H. Ochoa, F. Guinea, B. Özyilmaz, B. J. van Wees, and I. J. Vera-Marun, “Colloquium: Spintronics in graphene and other two-dimensional materials,” *Rev. Mod. Phys.* **92**, 021003 (2020).
- [198] T. Jungwirth, X. Marti, P. Wadley, and J. Wunderlich, “Antiferromagnetic spintronics,” *Nature Nanotechnology* **11**, 231–241 (2016).
- [199] Rodrigo G. Pereira and Reinhold Egger, “Electrical access to ising anyons in kitaev spin liquids,” *Phys. Rev. Lett.* **125**, 227202 (2020).
- [200] David Aasen, Roger S. K. Mong, Benjamin M. Hunt, David Mandrus, and Jason Alicea, “Electrical probes

- of the non-abelian spin liquid in kitaev materials,” *Phys. Rev. X* **10**, 031014 (2020).
- [201] Titus Neupert, Luiz Santos, Claudio Chamon, and Christopher Mudry, “Fractional quantum hall states at zero magnetic field,” *Phys. Rev. Lett.* **106**, 236804 (2011).
- [202] Zhao Liu, Ahmed Abouelkomsan, and Emil J. Bergholtz, “Gate-tunable fractional chern insulators in twisted double bilayer graphene,” *Phys. Rev. Lett.* **126**, 026801 (2021).
- [203] Patrick J. Ledwith, Grigory Tarnopolsky, Eslam Khalaf, and Ashvin Vishwanath, “Fractional chern insulator states in twisted bilayer graphene: An analytical approach,” *Phys. Rev. Research* **2**, 023237 (2020).
- [204] Cécile Repellin and T. Senthil, “Chern bands of twisted bilayer graphene: Fractional Chern insulators and spin phase transition,” *Phys. Rev. Research* **2**, 023238 (2020).
- [205] Roger S. K. Mong, David J. Clarke, Jason Alicea, Natan H. Lindner, Paul Fendley, Chetan Nayak, Yuval Oreg, Ady Stern, Erez Berg, Kirill Shtengel, and Matthew P. A. Fisher, “Universal topological quantum computation from a superconductor-Abelian quantum Hall heterostructure,” *Phys. Rev. X* **4**, 011036 (2014).
- [206] Jason Alicea and Paul Fendley, “Topological phases with parafermions: Theory and blueprints,” *Annu. Rev. Condens. Matter Phys.* **7**, 119–139 (2016).